Supporting information

Highly Active Rare-Earth Metal Catalysts for Heteroselective Ring-Opening Polymerization of Racemic Lactide

Yu Pan,[a] Wenqiang Li,[a] Ning-Ning Wei,[b] Yat-Ming So,[c] Xiaoling Lai,[a] Yang Li,*[a] Kang Jiang,[a] Gaohong He*[a]

[a] State Key Laboratory of Fine Chemicals, School of Petroleum and Chemical Engineering, Dalian University of Technology, Panjin, Liaoning 124221, China.

[b] School of Life Science and Medicine, Dalian University of Technology, Panjin, Liaoning 124221, China.

[c] Department of Chemistry, The Hong Kong University of Science and Technology, Clear Water Bay, Kowloon, Hong Kong, China.

*To whom correspondence should be addressed: E-mail: chyangli@dlut.edu.cn, hgaohong@dlut.edu.cn

Table of Contents

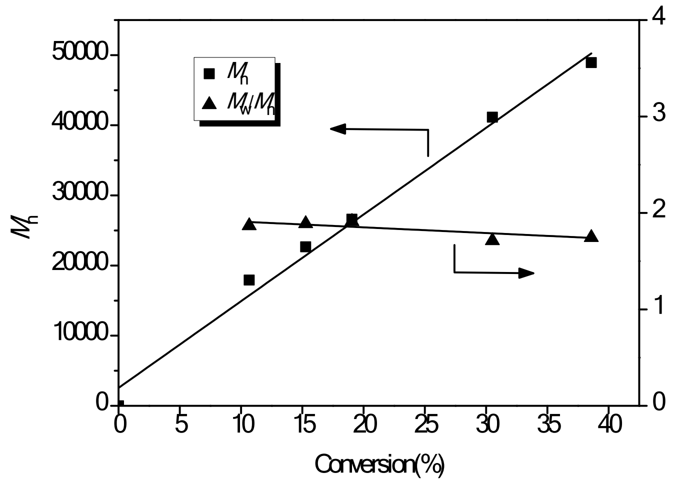

Fig. S1. Plot of molecular weights (M_n) and molecular weight distributions (M_w/M_n) against conversion for ROP of *rac*-LA using complex **2d** (Y) at [*rac*-LA]/[cat.] = 400 in THF.

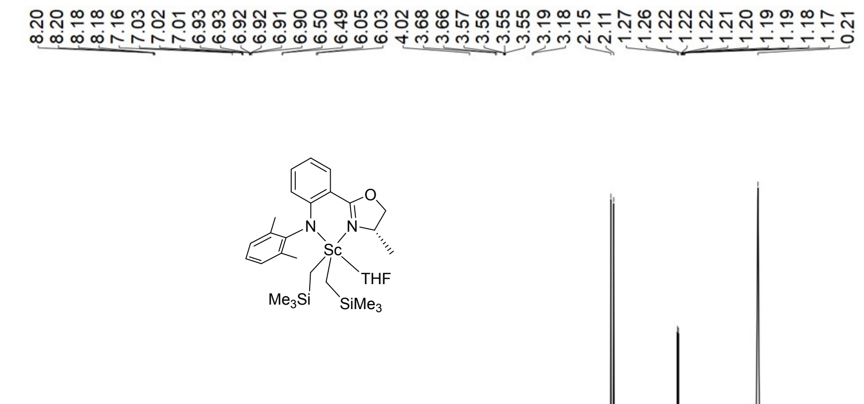

Fig. S2. ^{1}H NMR spectrum (500 MHz, C_6D_6, 25°C) of **L**^{a}-Sc(CH_2SiMe_3)$_2$THF (**1a**): δ 8.19 (dd, J = 8.2, 1.8 Hz, 1H, *o*-Ph*H*N), 7.02 (dd, J = 7.3, 1.9 Hz, 1H, *p*-Ph*H*N), 6.97 – 6.86 (m, 3H, *m*-NPhMe$_2$ and *m*-Ph*H*N), 6.50 (dd, J = 8.1, 6.9 Hz, 1H, *p*-NPhMe$_2$), 6.04 (d, J = 8.7 Hz, 1H, *m*-Ph*H*N), 4.80 – 4.68 (m, 1H, OCH$_2$C*H*N), 4.02 (t, J = 8.2 Hz, 1H, OC*H*$_2$CHN), 3.72 – 3.62 (m, 2H, THF), 3.56 (dd, J = 8.4, 3.4 Hz, 1H, OC*H*$_2$CHN), 3.18 (q, J = 7.1, 6.5 Hz, 2H, THF), 2.15 (s, 3H, NPh*Me$_2$*), 2.11 (s, 3H, NPh*Me$_2$*), 1.26 (d, J = 6.5 Hz, 3H, NCH*Me*), 1.25 – 1.14 (m, 4H, THF), 0.21 (s, 22H, C*H*$_2$Si*Me*$_3$) ppm.

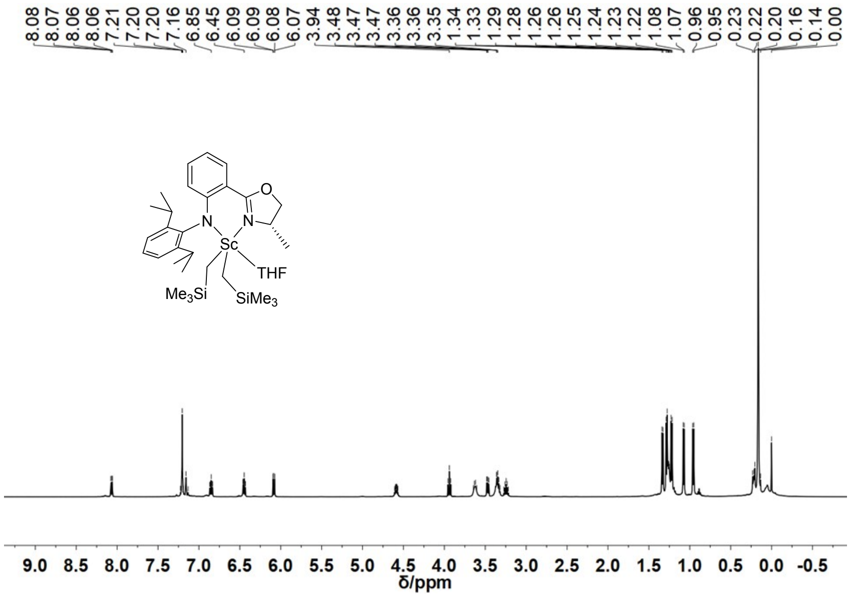

Fig. S3. ^{1}H NMR spectrum (500 MHz, C_6D_6, 25°C) of $\mathbf{L^b}$-Sc(CH_2SiMe_3)$_2$THF (**1b**): δ 8.07 (dd, J = 8.2, 1.8 Hz, 1H, *o*-Ph*H*N), 7.21 (d, J = 3.6 Hz, 3H, *p*-Ph*H*N and *m*-NPhCHMe$_2$), 6.85 (ddd, J = 8.7,6.8, 1.8 Hz, 1H, *m*-Ph*H*N), 6.45 (ddd, J = 8.0, 6.7, 1.1 Hz, 1H, *p*-NPhCHMe$_2$), 6.08 (dd, J = 8.9, 1.1 Hz, 1H, *m*-Ph*H*N), 4.59 (dddd, J = 8.5, 6.6, 4.3, 1.9 Hz, 1H, OCH$_2$C*H*N), 3.94 (t, J = 8.5 Hz, 1H, OC*H$_2$*CHN), 3.63 (q, J = 7.2, 6.8 Hz, 2H, THF), 3.47 (dd, J = 8.5, 4.8 Hz, 1H, OC*H$_2$*CHN), 3.41 – 3.29 (m, 3H, THF and NPhC*H*Me$_2$), 3.29 – 3.19 (m, 1H, NPhC*H*Me$_2$), 1.33 (d, J = 6.9 Hz, 3H, NPhCH*Me$_2$*), 1.28 (d, J = 6.9 Hz, 3H, NPhCH*Me$_2$*), 1.26(m, 4H, THF), 1.22 (d, J = 6.6 Hz, 3H, NPhCH*Me$_2$*), 1.07 (d, J = 6.7 Hz, 3H, NPhCH*Me$_2$*), 0.96 (d, J = 6.7 Hz, 3H, NCH*Me*), 0.25 – 0.19 (br, 2H, C*H$_2$*SiMe$_3$), 0.16 (s, 18H, CH$_2$Si*Me$_3$*), 0.05 (br, 2H, C*H$_2$*SiMe$_3$) ppm.

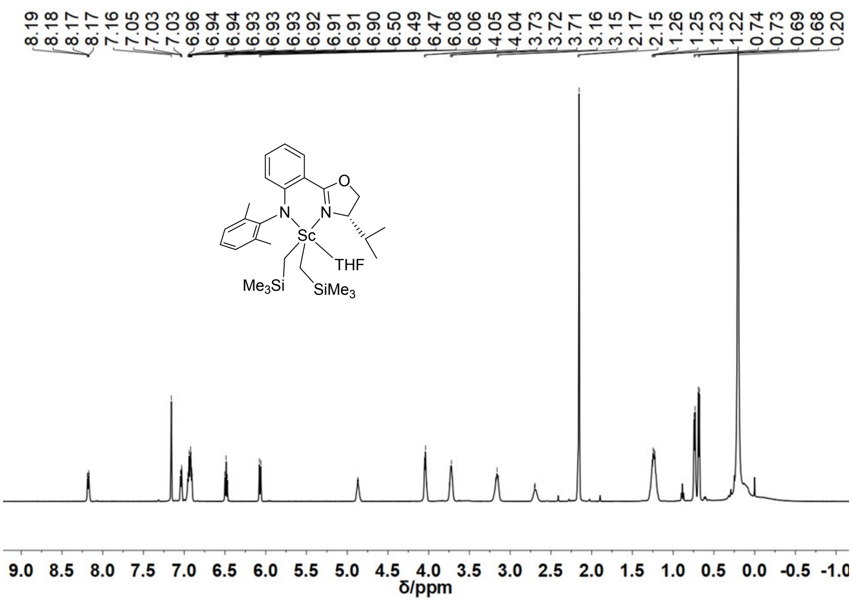

Fig. S4. ^{1}H NMR spectrum (500 MHz, C_6D_6, 25°C) of $\mathbf{L^c}$-Sc(CH_2SiMe_3)$_2$THF (**1c**): δ 8.18 (dd, J = 8.1, 1.9 Hz, 1H, *o*-Ph*H*N), 7.07 – 7.01 (m, 1H, *p*-Ph*H*N), 6.98 – 6.87 (m, 3H, *m*-NPhMe$_2$ and *m*Ph*H*N), 6.49 (t, J = 7.5 Hz, 1H, *p*-NPhMe$_2$), 6.07 (d, J = 8.8 Hz, 1H, *m*Ph*H*N), 4.86 (tq, J = 9.7, 5.4, 4.4 Hz, 1H, OCH$_2$C*H*N), 4.05 (d, J = 6.5 Hz, 2H, OC*H$_2$*CHN), 3.72 (t, J = 6.8 Hz, 2H, THF), 3.15 (q, J = 7.4, 6.0 Hz, 2H, THF), 2.76 – 2.59 (m, 1H, NCHC*H*Me$_2$), 2.15 (s, 6H, NPh*Me$_2$*), 1.24 (tq, J = 13.4, 6.5 Hz, 4H, THF), 0.74 (d, J = 6.8 Hz, 3H, NCHCH*Me$_2$*), 0.68 (d, J = 6.9 Hz, 3H, NCHCH*Me$_2$*), 0.20 (s, 18H, CH$_2$Si*Me$_3$*), 0.14 – 0.02 (br, 2H, C*H$_2$*SiMe$_3$), -0.10 (br, 2H, C*H$_2$*SiMe$_3$) ppm.

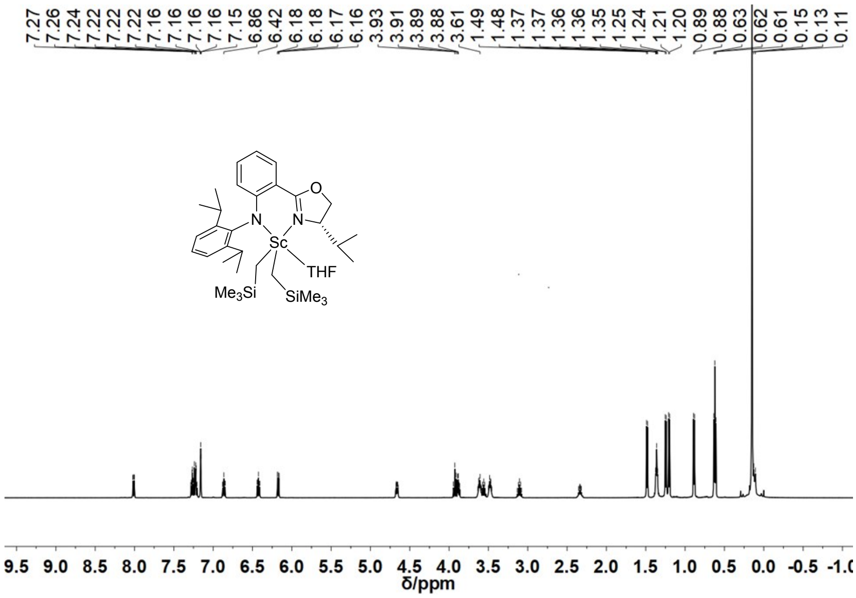

Fig. S5. [1]H NMR spectrum (500 MHz, C_6D_6, 25°C) of **L[d]**-Sc(CH_2SiMe_3)$_2$THF (**1d**): *δ* 8.01 (dd, *J* = 8.2, 1.8 Hz, 1H, *o*-Ph*H*N), 7.30 – 7.19 (m, 3H, *p*-Ph*H*N and *m*-NPhCHMe$_2$), 6.86 (ddd, *J* = 8.7, 6.8, 1.8 Hz, 1H, *m*-Ph*H*N), 6.42 (ddd, *J* = 8.0, 6.8, 1.1 Hz, 1H, *p*-NPhCHMe$_2$), 6.17 (dd, *J* = 8.7, 1.1 Hz, 1H, *m*-Ph*H*N), 4.66 (ddd, *J* = 9.0, 4.4, 3.5 Hz, 1H, OCH$_2$C*H*N), 3.93 (t, *J* = 9.1 Hz, 1H, OC*H$_2$*CHN), 3.88 (dd, *J* = 9.2, 4.5 Hz, 1H, OC*H$_2$*CHN), 3.65 – 3.58 (m, 2H, THF), 3.55 (q, *J* = 6.8 Hz, 1H, NPhC*H*Me$_2$), 3.51 – 3.43 (m, 2H, THF), 3.10 (p, *J* = 6.9 Hz, 1H, NPhC*H*Me$_2$), 2.34 (dd, *J* = 6.9, 3.5 Hz, 1H, NCHC*H*Me$_2$), 1.48 (d, *J* = 7.0 Hz, 3H, NPhCH*Me$_2$*), 1.40 – 1.31 (m, 4H, THF), 1.25 (d, *J* = 6.9 Hz, 3H, NPhCH*Me$_2$*), 1.20 (d, *J* = 6.7 Hz, 3H, NPhCH*Me$_2$*), 0.89 (d, *J* = 6.8 Hz, 3H, NPhCH*Me$_2$*), 0.62 (t, *J* = 6.6 Hz, 6H, NCHCH*Me$_2$*), 0.18 – 0.10 (m, 4H, C*H$_2$*SiMe$_3$), 0.15 (s, 18H, CH$_2$SiMe$_3$) ppm.

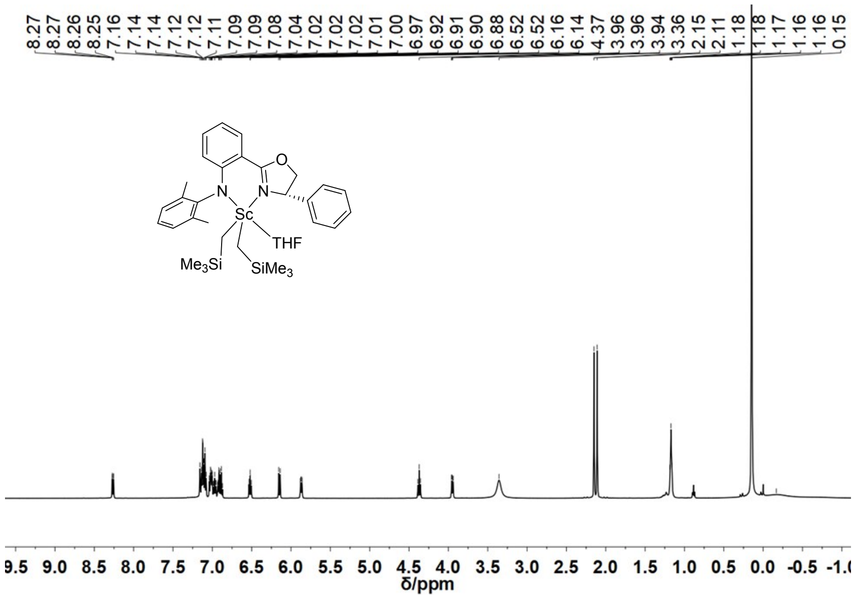

Fig. S6. [1]H NMR spectrum (500 MHz, C_6D_6, 25°C) of **L[e]**-Sc(CH_2SiMe_3)$_2$THF (**1e**): *δ* 8.26 (dd, *J* = 8.1, 1.8 Hz, 1H, *o*-Ph*H*N), 7.15 – 7.07 (m, 4H, NCH*Ph*), 7.02 (ddt, *J* = 8.8, 7.2, 1.7 Hz, 2H, *p*-Ph*H*N and *m*-NPhMe$_2$), 6.97 (ddd, *J* = 8.7, 6.7, 1.8 Hz, 1H, *m*-NPhMe$_2$), 6.94– 6.86 (m, 2H, NCH*Ph* and *m*-Ph*H*N), 6.52 (dd, *J* = 8.1, 6.8 Hz, 1H, *p*NPhMe$_2$), 6.15 (d, *J* = 8.8 Hz, 1H, *m*-Ph*H*N), 5.87 (dd, *J* = 8.5, 2.5 Hz, 1H, OCH$_2$C*H*N), 4.37 (t, *J* = 8.5 Hz, 1H, OC*H$_2$*CHN), 3.95 (dd, *J* = 8.4, 2.6 Hz, 1H, OC*H$_2$*CHN), 3.36 (s, 4H, THF), 2.15 (s, 3H, NPh*Me$_2$*), 2.11 (s, 3H, NPh*Me$_2$*), 1.21 – 1.12 (m, 4H, THF), 0.15 (s, 18H, CH$_2$Si*Me$_3$*), -0.17 (br, 4H, C*H$_2$*SiMe$_3$) ppm.

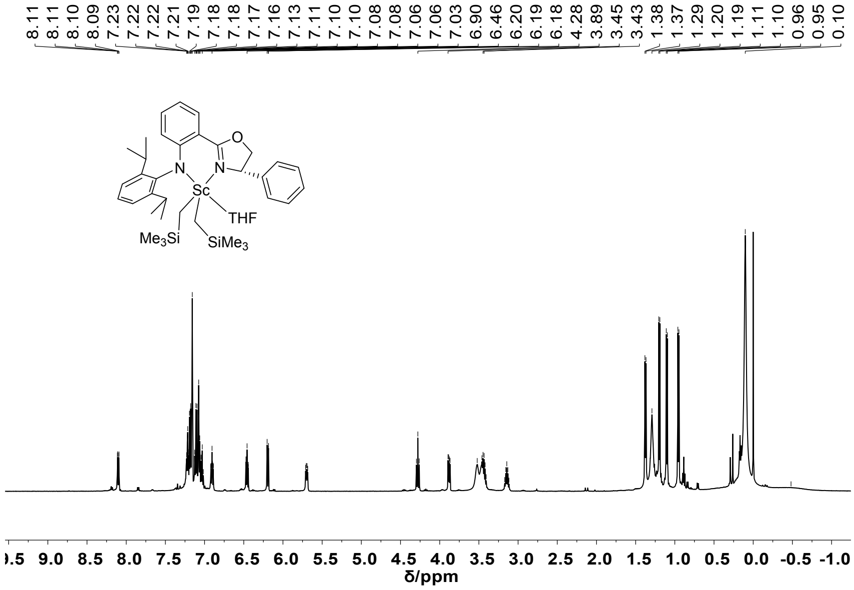

Fig. S7. ^{1}H NMR spectrum (500 MHz, C_6D_6, 25°C) of $\mathbf{L^f}$-Sc(CH_2SiMe_3)$_2$THF (**1f**): δ 8.10 (dd, J = 8.2, 1.8 Hz, 1H, *o*-Ph*H*N), 7.25 – 7.17 (m, 2H, NCH*Ph*), 7.14 – 7.05 (m, 5H, NCH*Ph and p*-PhHN and *m*-NPhC*H*Me$_2$), 7.05 – 7.01 (m, 1H, *m*-NPhC*H*Me$_2$), 6.91 (ddd, J = 8.7, 6.7, 1.8 Hz, 1H, *m*-Ph*H*N), 6.51 – 6.41 (m, 1H, *p*-NPhC*H*Me$_2$), 6.22 – 6.16 (m, 1H, *m*-Ph*H*N), 5.70 (dd, J = 9.0, 4.2 Hz, 1H, OCH$_2$C*H*N), 4.28 (t, J = 8.8 Hz, 1H, OC*H$_2$*CHN), 3.88 (dd, J = 8.7, 4.3 Hz, 1H, OC*H$_2$*CHN), 3.67 – 3.33 (m, 5H, THF and NPhC*H*Me$_2$), 3.24 – 3.06 (m, 1H, NPhC*H*Me$_2$), 1.38 (d, J = 6.9 Hz, 3H, NPhCH*Me$_2$*), 1.33 – 1.25 (m, 4H, THF), 1.20 (d, J = 6.6 Hz, 3H, NPhCH*Me$_2$*), 1.10 (d, J = 6.9 Hz, 3H, NPhCH*Me$_2$*), 0.95 (d, J = 6.8 Hz, 3H, NPhCH*Me$_2$*), 0.10 (s, 18H, CH$_2$Si*Me$_3$*), -0.48 (br, 4H, C*H$_2$*SiMe$_3$) ppm.

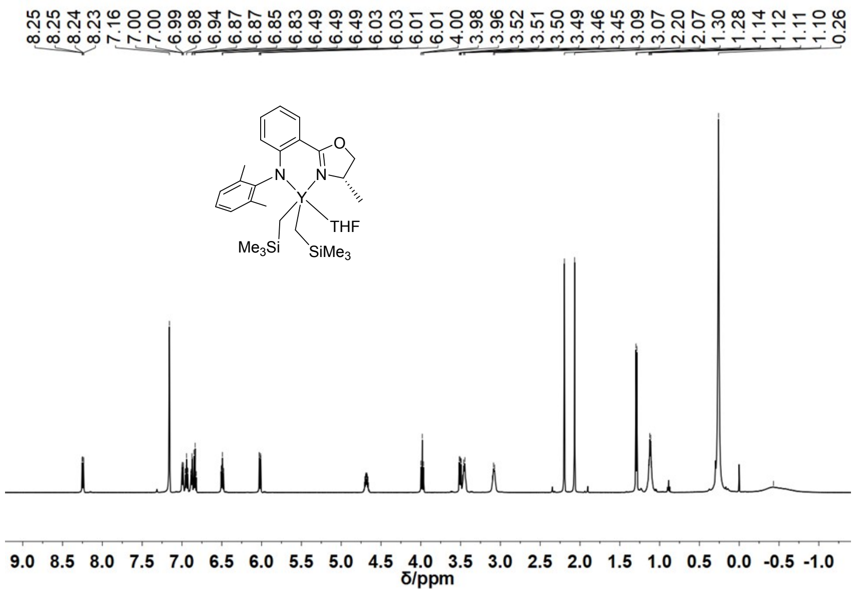

Fig. S8. ^{1}H NMR spectrum (500 MHz, C_6D_6, 25°C) of $\mathbf{L^a}$-Y(CH_2SiMe_3)$_2$THF (**2a**): δ 8.24 (dd, J = 8.2, 1.8 Hz, 1H, *o*-Ph*H*N), 6.99 (dd, J = 7.4, 1.8 Hz, 1H, *p*-Ph*H*N), 6.94 (ddd, J = 8.6, 6.7, 1.8 Hz, 1H, *m*-NPhMe$_2$), 6.88 (dd, J = 7.7, 1.8 Hz, 1H, *m*-NPhMe$_2$), 6.83 (t, J = 7.4 Hz, 1H, *m*-Ph*H*N), 6.49 (ddd, J = 8.1, 6.7, 1.2 Hz, 1H, *p*-NPhMe$_2$), 6.02 (dd, J = 8.7, 1.1 Hz, 1H, *m*-Ph*H*N), 4.68 (dqd, J = 8.4, 6.6, 4.3 Hz, 1H, OCH$_2$C*H*N), 3.98 (t, J = 8.4 Hz, 1H, OC*H$_2$*CHN), 3.50 (dd, J = 8.4, 4.4 Hz, 1H, OC*H$_2$*CHN), 3.45 (q, J = 6.8 Hz, 2H, THF), 3.08 (d, J = 7.1 Hz, 2H, THF), 2.20 (s, 3H, NPh*Me$_2$*), 2.07 (s, 3H, NPh*Me$_2$*), 1.29 (d, J = 6.6 Hz, 4H, NCH*Me*), 1.12 (q, J = 6.0 Hz, 4H, THF), 0.26 (s, 18H, CH$_2$Si*Me$_3$*), -0.44 (br, 4H, C*H$_2$*SiMe$_3$) ppm.

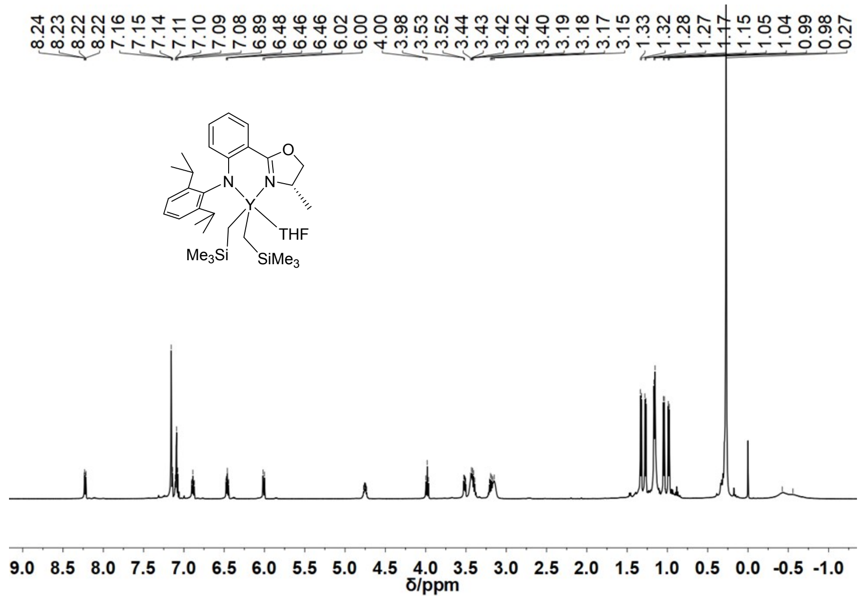

Fig. S9. ^{1}H NMR spectrum (500 MHz, C_6D_6, 25°C) of $\mathbf{L^b}$-Y(CH_2SiMe_3)$_2$THF (**2b**): δ 8.23 (dd, J = 8.2, 1.8 Hz, 1H, *o*-Ph*H*N), 7.14 (d, J = 2.4 Hz, 1H, *p*-Ph*H*N), 7.12 – 7.05 (m, 2H, *m*-NPhCHMe$_2$), 6.89 (ddd, J = 8.7, 6.7, 1.9 Hz, 1H, *m*-Ph*H*N), 6.46 (ddd, J = 8.1, 6.7, 1.1 Hz, 1H, *p*-NPhCHMe$_2$), 6.01 (d, J = 8.7 Hz, 1H, *m*-Ph*H*N), 4.84 – 4.66 (m, 1H, OCH$_2$C*H*N), 3.98 (t, J = 8.2 Hz, 1H, OC*H$_2$*CHN), 3.51 (dd, J = 8.3, 4.2 Hz, 1H, OC*H$_2$*CHN), 3.41 (ddd, J = 20.4, 8.4, 5.5 Hz, 3H, NPhC*H*Me$_2$ and THF), 3.19 (td, J = 15.7, 14.6, 7.9 Hz, 3H, NPhC*H*Me$_2$ and THF), 1.33 (d, J = 6.6 Hz, 3H, NPhCH*Me$_2$*), 1.27 (d, J = 6.9 Hz, 3H, NPhCH*Me$_2$*), 1.16 (d, J = 6.9 Hz, 7H, NPhCH*Me$_2$* and THF), 1.04 (d, J = 6.7 Hz, 3H, NPhCH*Me$_2$*), 0.98 (d, J = 6.7 Hz, 3H, NCH*Me*), 0.27 (s, 18H, CH$_2$Si*Me$_3$*), -0.43 (br, 2H, C*H$_2$*SiMe$_3$), -0.56 (br, 2H, C*H$_2$*SiMe$_3$) ppm.

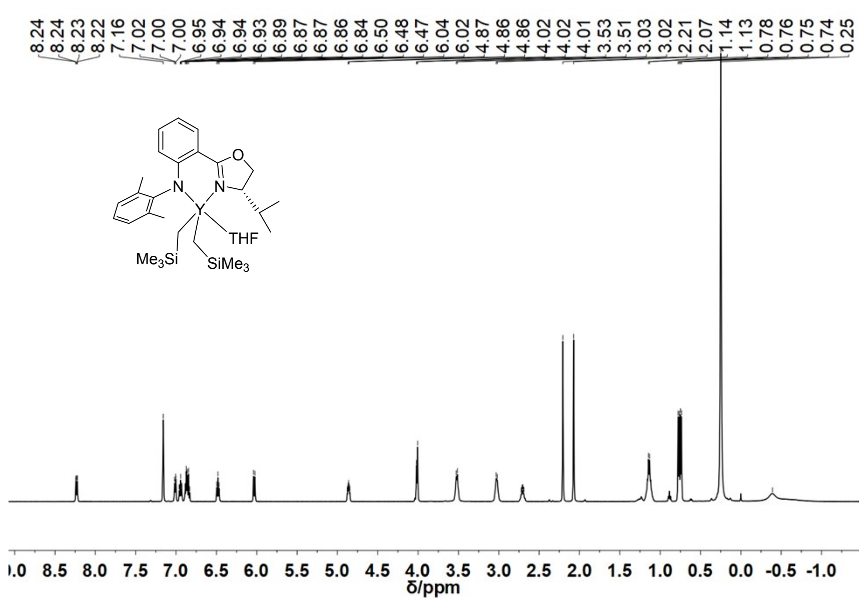

Fig. S10. ^{1}H NMR spectrum (500 MHz, C_6D_6, 25°C) of $\mathbf{L^c}$-Y(CH_2SiMe_3)$_2$THF (**2c**): δ 8.23 (dd, J = 8.2, 1.9 Hz, 1H, *o*-Ph*H*N), 7.06 – 6.98 (m, 1H, *p*-Ph*H*N), 6.94 (ddd, J = 8.8, 6.7, 1.9 Hz, 1H, *m*NPhMe$_2$), 6.91 – 6.82 (m, 2H, *m*-NPhMe$_2$ and *m*-Ph*H*N), 6.48 (t, J = 7.5 Hz, 1H, *p*-NPhMe$_2$), 6.03 (d, J = 8.7 Hz, 1H, *m*-Ph*H*N), 4.86 (ddd, J = 8.0, 5.6, 3.3 Hz, 1H, OCH$_2$C*H*N), 4.05 – 3.96 (m, 2H, OC*H$_2$*CHN), 3.52 (q, J = 6.7 Hz, 2H, THF), 3.03 (q, J = 6.7 Hz, 2H, THF), 2.71 (td, J = 6.9, 3.4 Hz, 1H, NCHC*H*Me$_2$), 2.21 (s, 3H, NPh*Me$_2$*), 2.07 (s, 3H, NPh*Me$_2$*), 1.14 (h, J = 6.4 Hz, 4H, THF), 0.76 (dd, J = 14.1, 6.9 Hz, 6H, NCHCH*Me$_2$*), 0.25 (s, 18H, CH$_2$Si*Me$_3$*), -0.39 (br, 4H, C*H$_2$*SiMe$_3$) ppm.

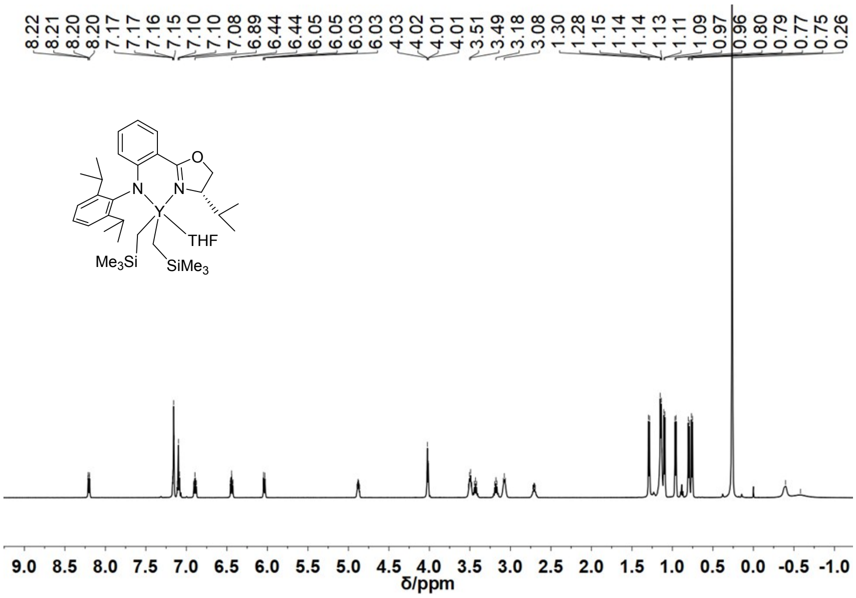

Fig. S11. ^{1}H NMR spectrum (500 MHz, C_6D_6, 25°C) of **L^d**-Y(CH_2SiMe_3)$_2$THF (**2d**): δ 8.21 (dd, J = 8.2, 1.9 Hz, 1H, *o*-Ph*H*N), 7.17 (d, J = 2.8 Hz, 1H, *p*-Ph*H*N), 7.14 – 7.04 (m, 2H, *m*-NPhCHMe$_2$), 6.89 (ddd, J = 8.7, 6.7, 1.9 Hz, 1H, *m*-Ph*H*N), 6.44 (ddd, J = 8.0, 6.7, 1.1 Hz, 1H, *p*-NPhCHMe$_2$), 6.04 (dd, J = 8.7, 1.2 Hz, 1H, *m*-Ph*H*N), 4.88 (ddd, J = 7.2, 5.6, 3.3 Hz, 1H, OCH$_2$C*H*N), 4.06 – 3.98 (m, 2H, OC*H$_2$*CHN), 3.50 (q, J = 6.9 Hz, 2H, THF), 3.43 (p, J = 6.8 Hz, 1H, NPhC*H*Me$_2$), 3.18 (p, J = 6.8 Hz, 1H, NPhC*H*Me$_2$), 3.08 (t, J = 6.5 Hz, 2H, THF), 2.71 (ddd, J = 10.2, 6.4, 2.9 Hz, 1H, NCHC*H*Me$_2$), 1.29 (d, J = 6.9 Hz, 3H, NPhCH*Me$_2$*), 1.14 (dd, J = 6.4, 3.4 Hz, 7H, NPhCH*Me$_2$* and THF), 1.10 (d, J = 6.7 Hz, 3H, NPhCH*Me$_2$*), 0.96 (d, J = 6.7 Hz, 3H, NPhCH*Me$_2$*), 0.80 (dd, J = 7.0, 2.1 Hz, 3H, NCHCH*Me$_2$*), 0.76 (d, J = 6.8 Hz, 3H, NCHCH*Me$_2$*), 0.26 (s, 18H, CH$_2$Si*Me$_3$*), -0.39 (br, 2H, C*H$_2$*SiMe$_3$),-0.57 (br, 2H, C*H$_2$*SiMe$_3$) ppm.

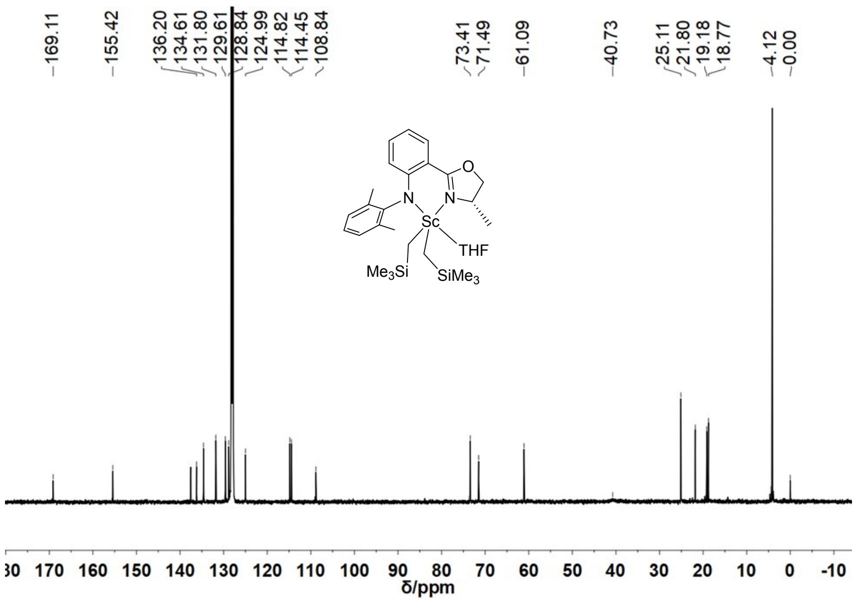

Fig. S12. ^{13}C NMR spectrum (125 MHz, C_6D_6, 25°C) of **L^a**-Sc(CH_2SiMe_3)$_2$THF (**1a**): δ 169.11 (s, O*C*N), 155.42 , 137.53 , 136.20 , 134.61 , 131.80 , 129.61 , 128.84 , 124.99 , 114.82 , 114.45 , 108.84 , 73.41 (s, THF), 71.49 (s, O*C*H$_2$CH), 61.09 (s, OCH$_2$*C*H), 40.73 (br, *C*H$_2$SiMe$_3$), 25.11 (s, THF), 21.80 (s, NPh*Me$_2$*), 19.18 (s, NPh*Me$_2$*), 18.77 (s, NCH*Me*), 4.12 (s, CH$_2$Si*Me$_3$*) ppm.

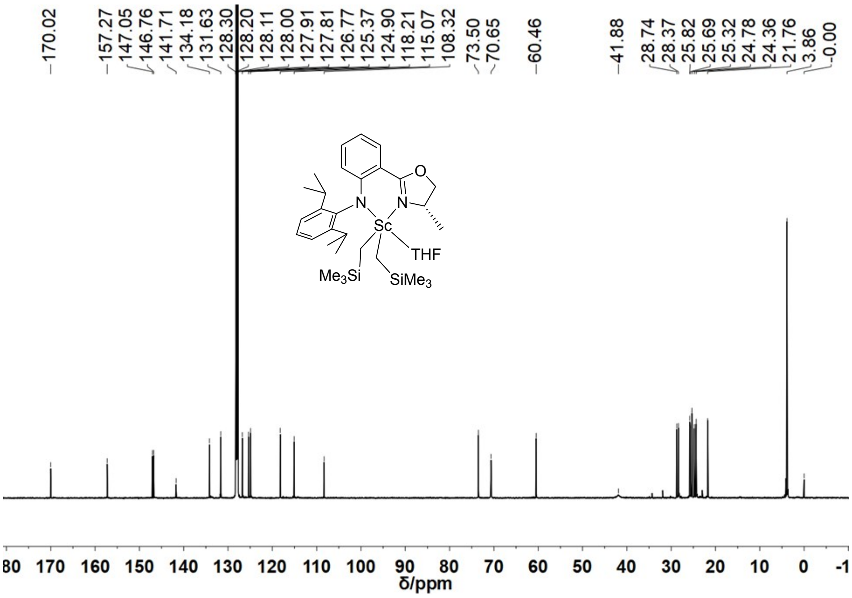

Fig. S13. ^{13}C NMR spectrum (125 MHz, C_6D_6, 25°C) of $\mathbf{L^b}$-Sc(CH_2SiMe_3)$_2$THF (**1b**): δ 170.02 (s, O*C*N), 157.27 , 147.05 , 146.76 , 141.71 , 134.18 , 131.63, 126.77 , 125.37 , 124.90 , 118.21 , 115.07 , 108.32 , 73.50 (s, THF), 70.65 (s, O*C*H_2CH), 60.46 (s, OCH_2*C*H), 41.88 (br, *C*H_2SiMe_3), 28.74 (s, NPh*C*HMe$_2$), 28.37 (s, NPh*C*HMe$_2$), 25.82 (s, NPhCH*Me$_2$*), 25.69 (s, NPhCH*Me$_2$*), 25.32 (s, THF), 24.78 (s,NPhCH*Me$_2$*), 24.36 (s, NPhCH*Me$_2$*), 21.76 (s, NCH*Me*), 3.86 (s, CH_2Si*Me$_3$*) ppm.

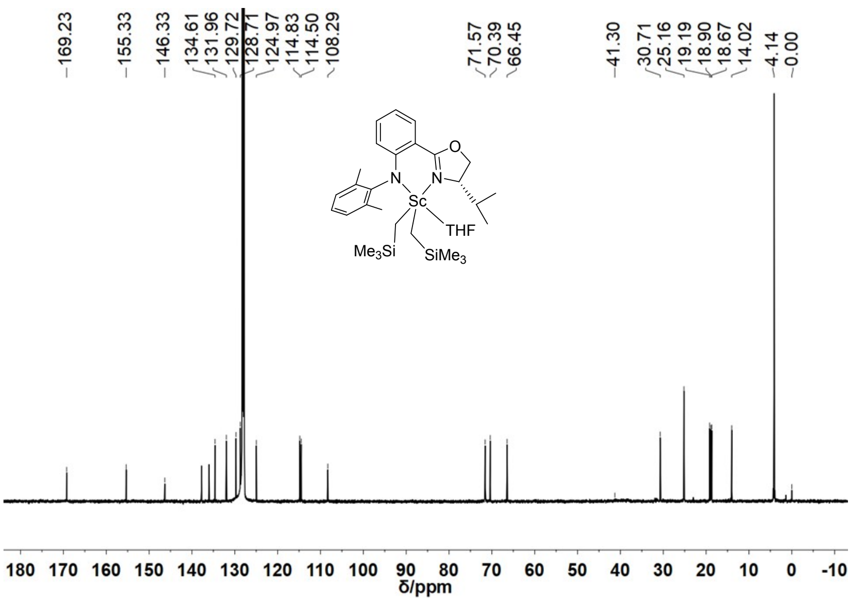

Fig. S14. ^{13}C NMR spectrum (125 MHz, C_6D_6, 25°C) of $\mathbf{L^c}$-Sc(CH_2SiMe_3)$_2$THF (**1c**): δ 169.23 (s, O*C*N), 155.33 , 146.33 , 137.76 , 136.02 , 134.61 , 131.96 , 129.72 , 128.71 , 124.97 , 114.83 , 114.50 , 108.29 , 71.57 (s, THF), 70.39 (s, O*C*H_2CH), 66.45 (s, OCH_2*C*H), 41.30 (br, *C*H_2SiMe_3), 30.71 (s, NCH*C*HMe$_2$), 25.16 (s, THF), 19.19 (s, NPh*Me$_2$*), 18.90 (s, NPh*Me$_2$*), 18.67 (s, NCHCH*Me$_2$*), 14.02 (s, NCHCH*Me$_2$*), 4.14 (s, CH_2Si*Me$_3$*) ppm.

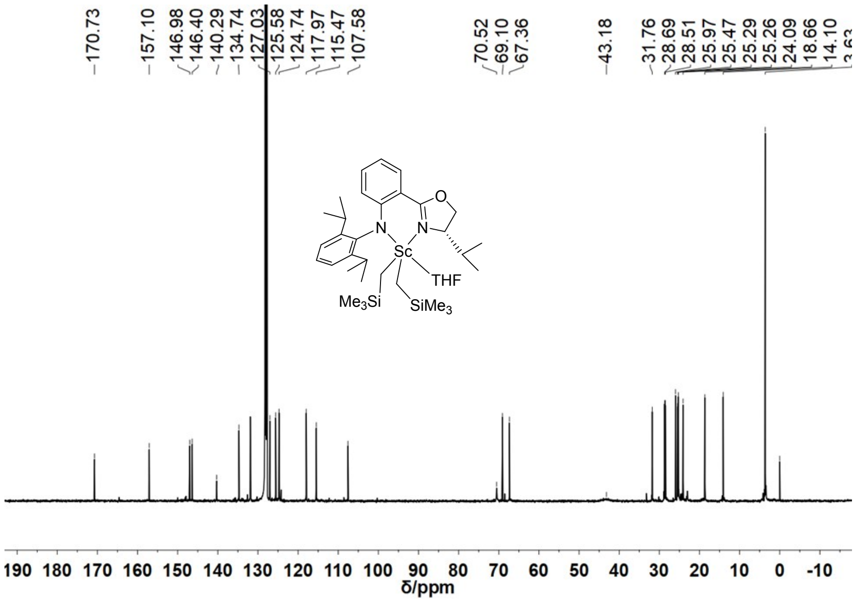

Fig. S15. ^{13}C NMR spectrum (125 MHz, C_6D_6, 25°C) of **L^d**-Sc(CH_2SiMe_3)$_2$THF (**1d**): δ 170.73 (s, O*C*N), 157.10 , 146.98 , 146.40 , 140.29 , 134.74 , 131.89 , 127.03 , 125.58 , 124.74 , 117.97 , 115.47 , 107.58 , 70.52 (s, THF), 69.10 (s, O*C*H_2CH), 67.36 (s, OCH_2*C*H), 43.18 (br, *C*H_2SiMe_3), 31.76 (s, NCH*C*HMe$_2$), 28.69 (s, NPh*C*HMe$_2$), 28.51 (s, NPh*C*HMe$_2$), 25.97 (s, NPhCH*Me$_2$*), 25.47 (s, THF), 25.28 (d, *J* = 4.6 Hz, NPhCH*Me$_2$*), 24.09 (s, NPhCH*Me$_2$*), 18.66 (s, NCHCH*Me$_2$*), 14.10 (s, NCHCH*Me$_2$*), 3.63 (s, CH_2Si*Me$_3$*) ppm.

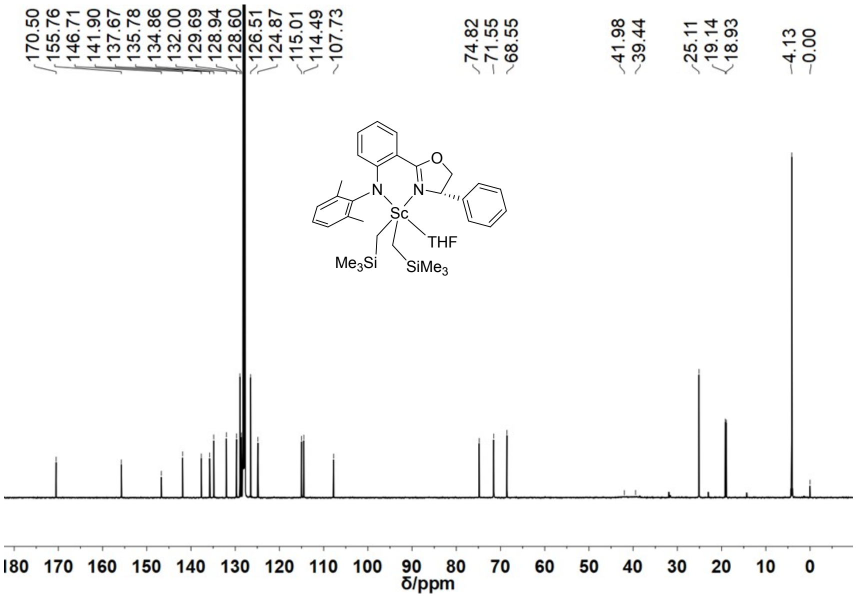

Fig. S16. ^{13}C NMR spectrum (125 MHz, C_6D_6, 25°C) of **L^e**-Sc(CH_2SiMe_3)$_2$THF (**1e**): δ 170.50 (s, O*C*N), 155.76 , 146.71 , 141.90 , 137.67 , 135.78 , 134.86 , 132.00 , 129.69 , 128.94 , 128.60 , 126.51 , 124.87 , 115.01 , 114.49 , 107.73 , 74.82 (s, THF), 71.55 (s, O*C*H_2CH), 68.55 (s, OCH_2*C*H), 41.98 (br, *C*H_2SiMe_3), 39.44 (br, *C*H_2SiMe_3), 25.11 (s, THF), 19.14 (s, NPh*Me$_2$*), 18.93 (s, NPh*Me$_2$*), 4.13 (s, CH_2Si*Me$_3$*) ppm.

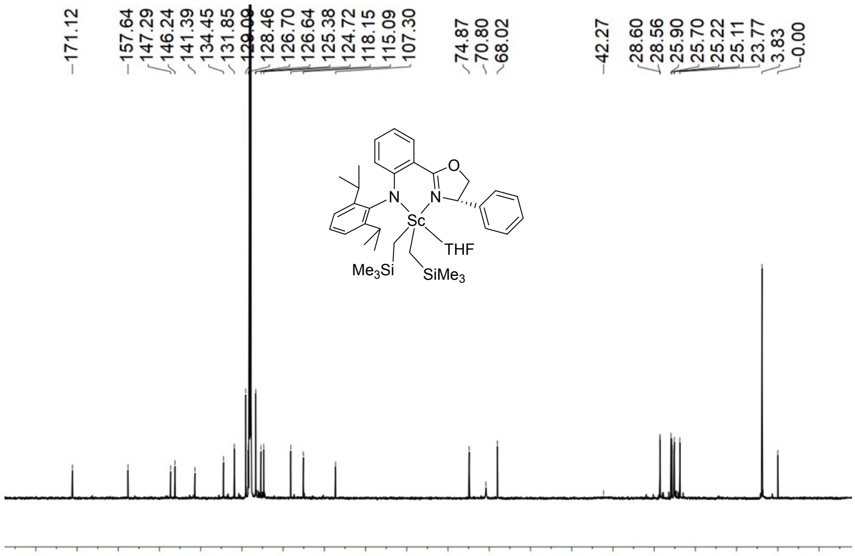

Fig. S17. ^{13}C NMR spectrum (125 MHz, C_6D_6, 25°C) of $\mathbf{L^f}$-Sc(CH_2SiMe_3)$_2$THF (**1f**): δ 171.12 (s, O*C*N), 157.64 , 147.29 , 146.24 , 141.39 , 134.45 ,131.85 , 129.09 , 128.46 , 126.67 (d, J = 7.1 Hz), 125.38 , 124.72 , 118.15 , 115.09 , 107.30 , 74.87 (s, THF), 70.80 (s, O*C*H_2CH), 68.02 (s, OCH_2*C*H), 42.27 (br, *C*H_2SiMe_3), 28.58 (d, J = 5.1 Hz, N*C*HPh*Me$_2$*),25.90 (s, N*C*HPh*Me$_2$*), 25.70 (s, THF), 25.17 (d, J = 13.6 Hz, NCHPh*Me$_2$*), 23.77 (s, NCHPh*Me$_2$*), 3.83 (s, CH_2Si*Me$_3$*) ppm.

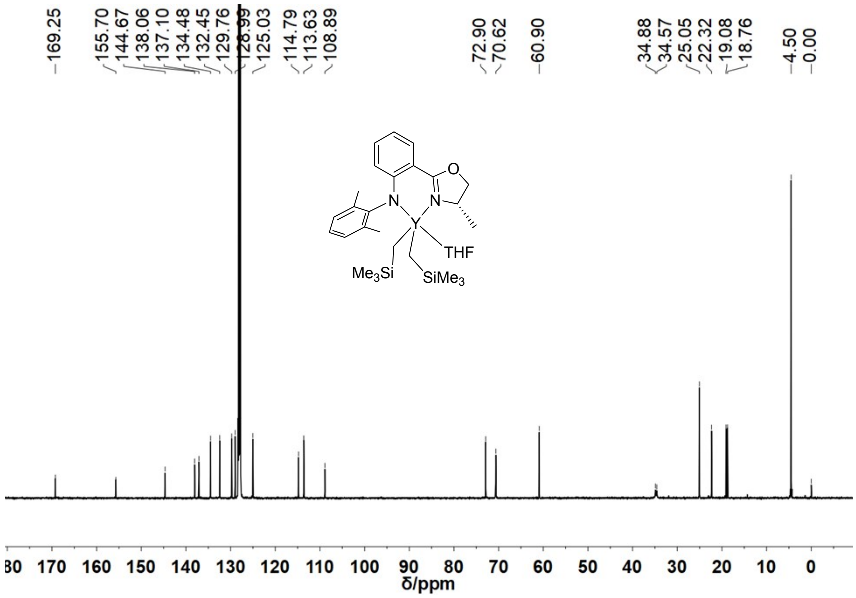

Fig. S18. ^{13}C NMR spectrum (125 MHz, C_6D_6, 25°C) of $\mathbf{L^a}$-Y(CH_2SiMe_3)$_2$THF (**2a**): δ 169.24 (s, O*C*N), 155.71 , 144.67 , 138.06 , 137.10 , 134.48 , 132.45 , 129.76 , 128.99 , 125.03 , 114.79 , 113.63 , 108.89 , 72.90 (s, THF), 70.62 (s, O*C*H_2CH), 60.90 (s, OCH_2*C*H), 34.73 (d, J = 38.9 Hz, *C*H_2SiMe_3), 25.05 (s, THF), 22.32 (s, NPh*Me$_2$*), 19.08 (s, NPh*Me$_2$*), 18.76 (s, NCH*Me*), 4.50 (s, CH_2Si*Me$_3$*) ppm.

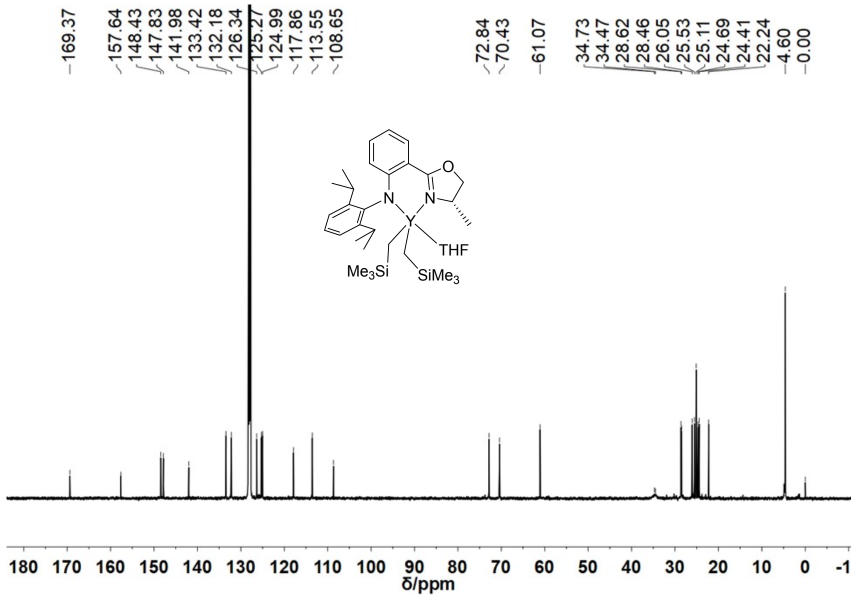

Fig. S19. ^{13}C NMR spectrum (125 MHz, C_6D_6, 25°C) of **L^{b}**-Y(CH_2SiMe_3)$_2$THF (**2b**): δ 169.37 (s, O*C*N), 157.64 , 148.43 , 147.83 , 141.98 , 133.42 , 132.18 , 126.34 , 125.27 , 124.99 , 117.86 , 113.55 , 108.65 , 72.84 (s, THF), 70.43 (s, O*C*H_2CH), 61.07 (s, OCH_2*C*H), 34.60 (d, *J* = 32.5 Hz, *C*H_2SiMe_3), 28.62 (s, NPh*C*HMe$_2$), 28.46 (s, NPh*C*HMe$_2$), 26.05 (s, NPhCH*Me$_2$*), 25.53 (s, NPhCH*Me$_2$*), 25.11 (s, THF), 24.69 (s, NPhCH*Me$_2$*), 24.41 (s, NPhCH*Me$_2$*), 22.24 (s, NCH*Me*), 4.60 (s, CH_2Si*Me$_3$*) ppm.

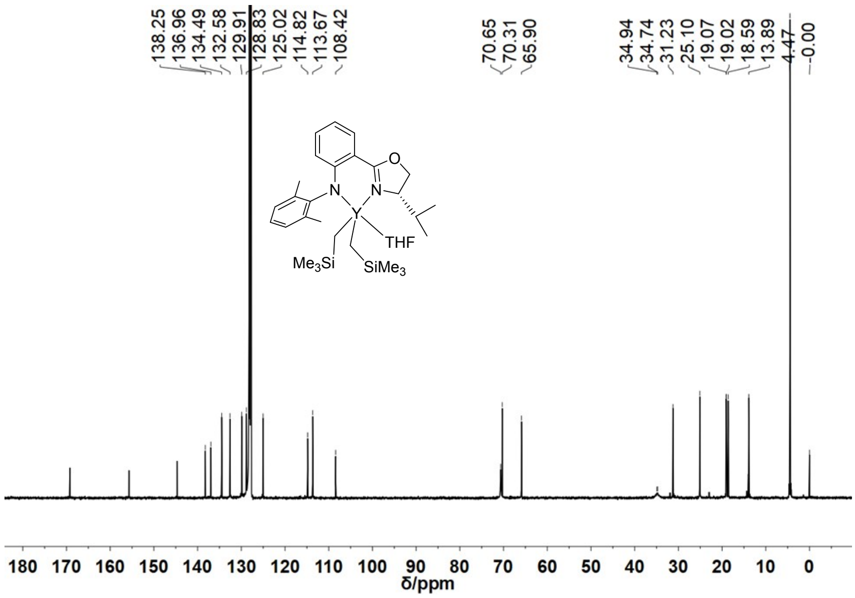

Fig. S20. ^{13}C NMR spectrum (125 MHz, C_6D_6, 25°C) of **L^{c}**-Y(CH_2SiMe_3)$_2$THF (**2c**): δ 169.21 (s, O*C*N), 155.71 , 144.66 , 138.25 , 136.96 , 134.49 , 132.58 , 129.91 , 128.83 , 125.02 , 114.82 , 113.67 , 108.42 , 70.65 (s, THF), 70.31 (s, O*C*H_2CH), 65.90 (s, OCH_2*C*H), 34.84 (d, *J* = 25.0 Hz, *C*H_2SiMe_3), 31.23 (s, NCH*C*HMe$_2$), 25.10 (s, THF), 19.04 (d, *J* = 6.6 Hz, NPh*Me$_2$*), 18.59 (s, NCHCH*Me$_2$*), 13.89 (s, NCHCH*Me$_2$*), 4.47 (s, CH_2Si*Me$_3$*) ppm.

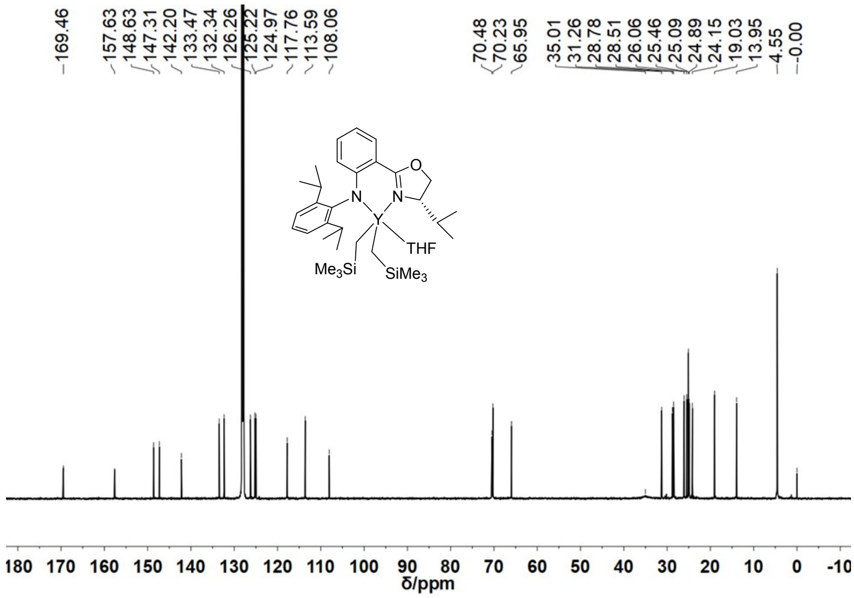

Fig. S21. ^{13}C NMR spectrum (125 MHz, C_6D_6, 25°C) of **L$^{\mathbf{d}}$**-Y(CH_2SiMe_3)$_2$THF (**2d**): *δ* 169.46 (s, O*C*N), 157.63 , 148.63 , 147.31 , 142.20 , 133.47 , 132.34 , 126.26 , 125.23 , 124.97 , 117.76 , 113.59 , 108.06 , 70.48 (s, THF), 70.23 (s, O*C*H$_2$CH), 65.95 (s, OCH$_2$*C*H), 35.01 (br, *C*H$_2$SiMe$_3$), 31.26 (s, NCH*C*HMe$_2$), 28.78 (s, NPh*C*HMe$_2$), 28.51 (s, NPh*C*HMe$_2$), 26.06 (s, NPhCH*Me$_2$*), 25.46 (s, NPhCH*Me$_2$*), 25.09 (s, THF), 24.89 (s, NPhCH*Me$_2$*), 24.15 (s, NPhCH*Me$_2$*), 19.03 (s, NCHCH*Me$_2$*), 13.95 (s, NCHCH*Me$_2$*), 4.55 (s, CH$_2$Si*Me$_3$*) ppm.

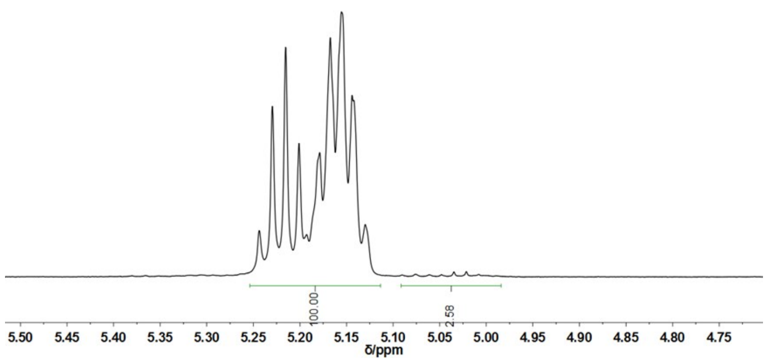

Fig. S22. ^{1}H NMR spectrum (500 MHz, $CDCl_3$, 25°C) of the resultant PLA (Table 1, run 1).

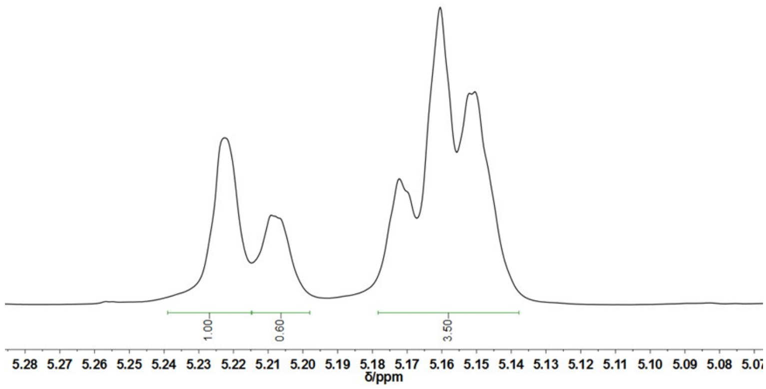

Fig. S23. Homonuclear decoupled ^{1}H NMR spectrum (500 MHz, $CDCl_3$, 25°C) of the resultant PLA (Table 1, run 1).

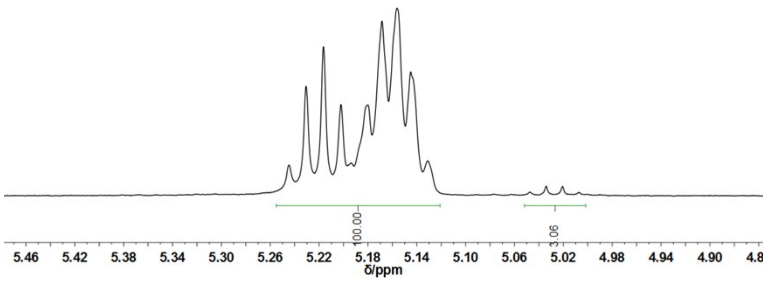

Fig. S24. ^{1}H NMR spectrum (500 MHz, $CDCl_3$, 25°C) of the resultant PLA (Table 1, run 2).

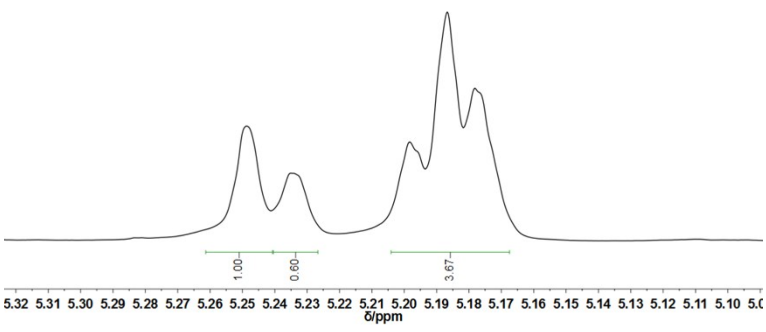

Fig. S25. Homonuclear decoupled ^{1}H NMR spectrum (500 MHz, $CDCl_3$, 25°C) of the resultant PLA (Table 1, run 2).

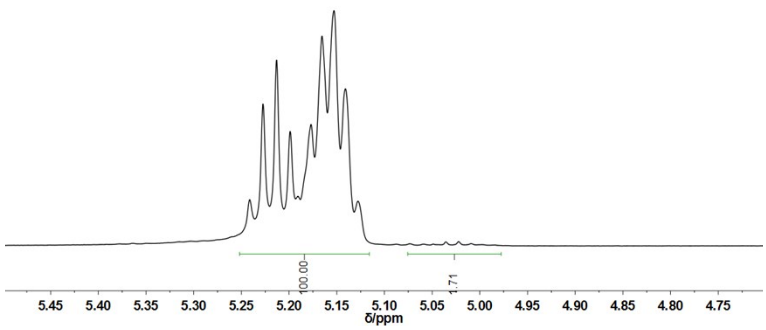

Fig. S26. ^{1}H NMR spectrum (500 MHz, $CDCl_3$, 25°C) of the resultant PLA (Table 1, run 3).

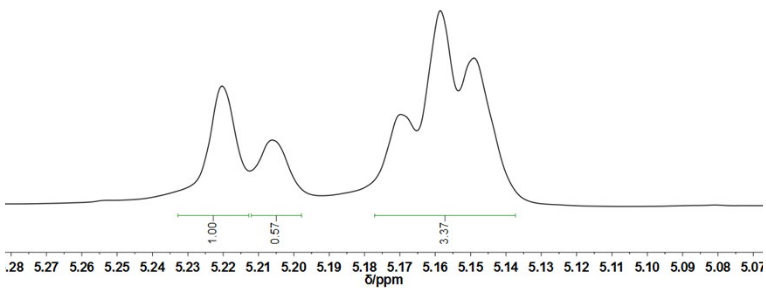

Fig. S27. Homonuclear decoupled ^{1}H NMR spectrum (500 MHz, $CDCl_3$, 25°C) of the resultant PLA (Table 1, run 3).

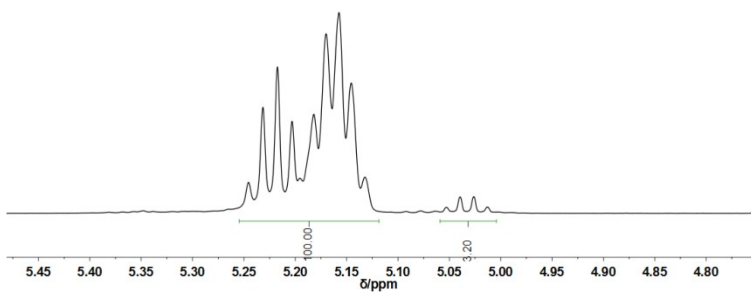

Fig. S28. ^{1}H NMR spectrum (500 MHz, $CDCl_3$, 25°C) of the resultant PLA (Table 1, run 4).

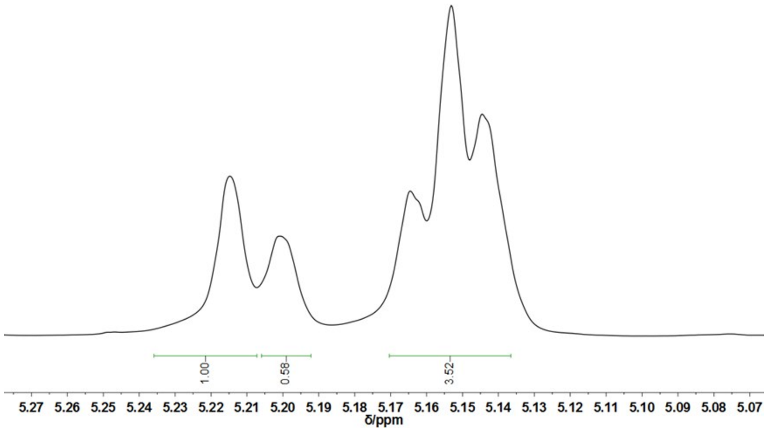

Fig. S29. Homonuclear decoupled ^{1}H NMR spectrum (500 MHz, $CDCl_3$, 25°C) of the resultant PLA (Table 1, run 4).

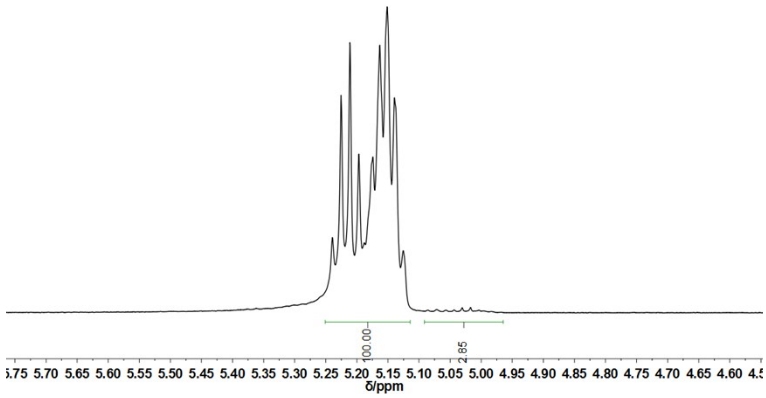

Fig. S30. ^{1}H NMR spectrum (500 MHz, $CDCl_3$, 25°C) of the resultant PLA (Table 1, run 5).

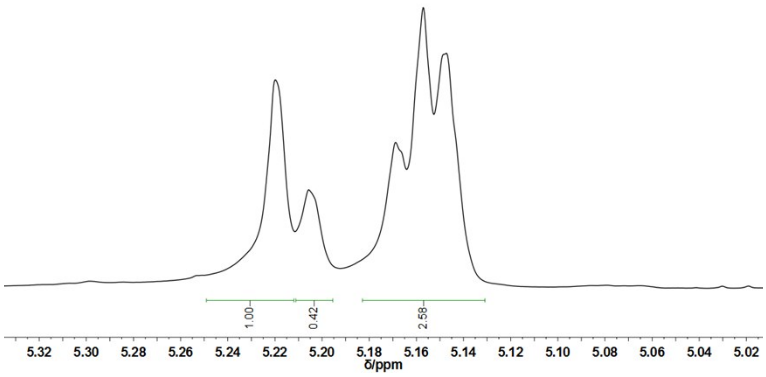

Fig. S31. Homonuclear decoupled ^{1}H NMR spectrum (500 MHz, $CDCl_3$, 25°C) of the resultant PLA (Table 1, run 5).

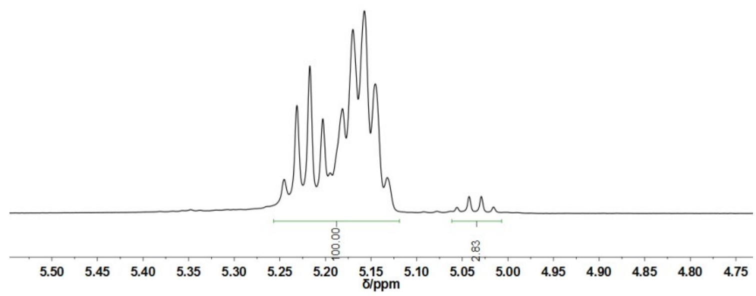

Fig. S32. ¹H NMR spectrum (500 MHz, $CDCl_3$, 25°C) of the resultant PLA (Table 1, run 6).

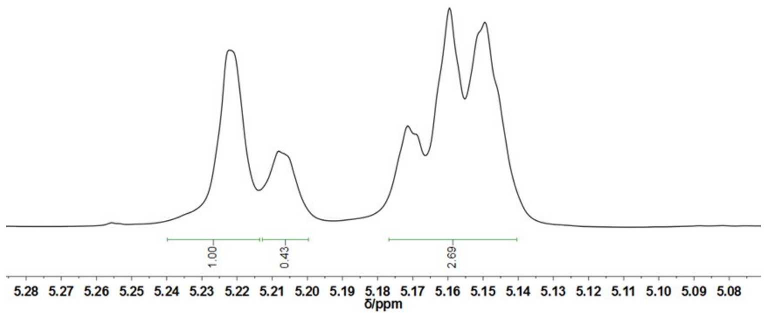

Fig. S33. Homonuclear decoupled ¹H NMR spectrum (500 MHz, $CDCl_3$, 25°C) of the resultant PLA (Table 1, run 6).

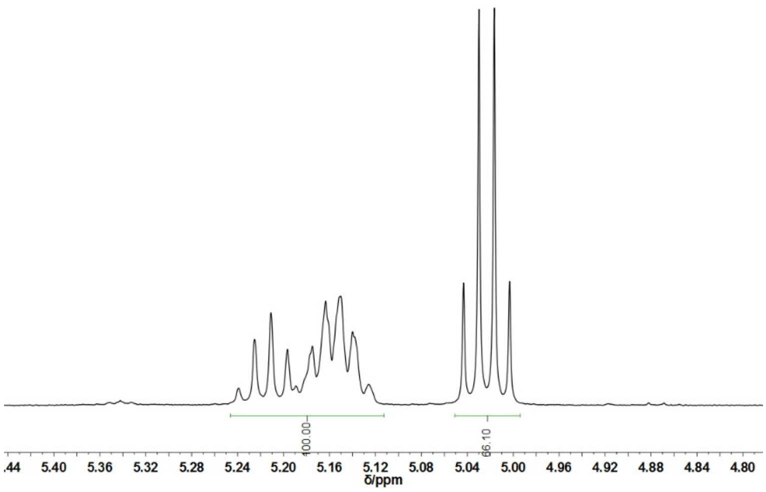

Fig. S34. ¹H NMR spectrum (500 MHz, $CDCl_3$, 25°C) of the resultant PLA (Table 1, run 7).

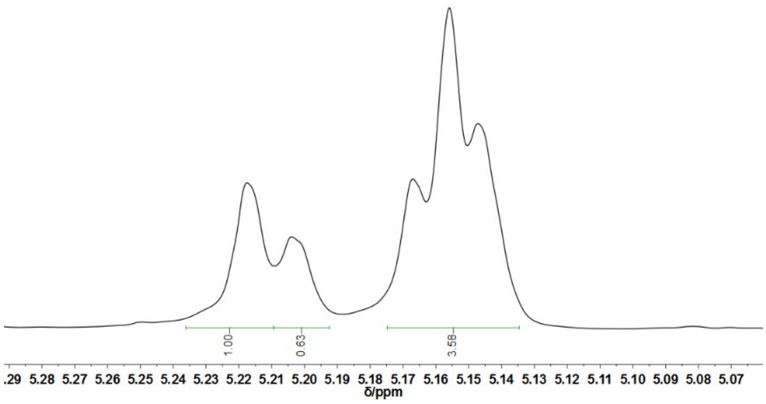

Fig. S35. Homonuclear decoupled ^{1}H NMR spectrum (500 MHz, $CDCl_3$, 25°C) of the resultant PLA (Table 1, run 7).

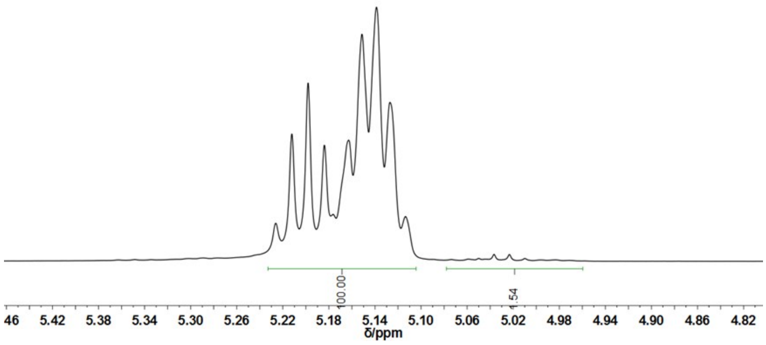

Fig. S36. ^{1}H NMR spectrum (500 MHz, $CDCl_3$, 25°C) of the resultant PLA (Table 1, run 8).

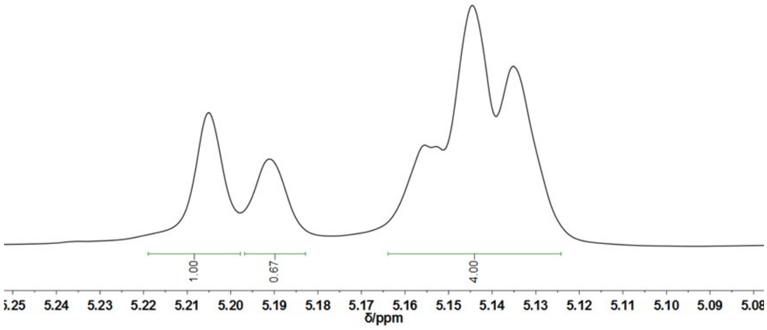

Fig. S37. Homonuclear decoupled ^{1}H NMR spectrum (500 MHz, $CDCl_3$, 25°C) of the resultant PLA (Table 1, run 8).

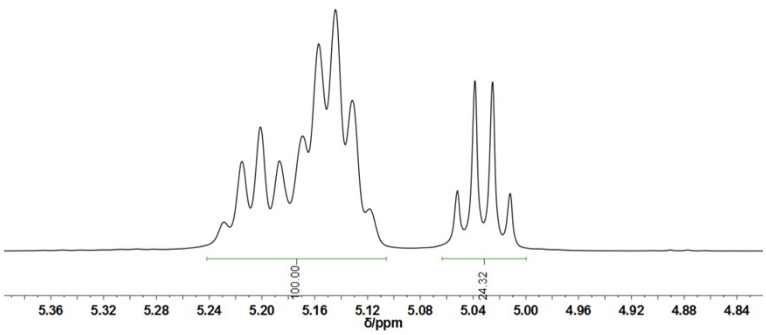

Fig. S38. ^{1}H NMR spectrum (500 MHz, $CDCl_3$, 25°C) of the resultant PLA (Table 1, run 9).

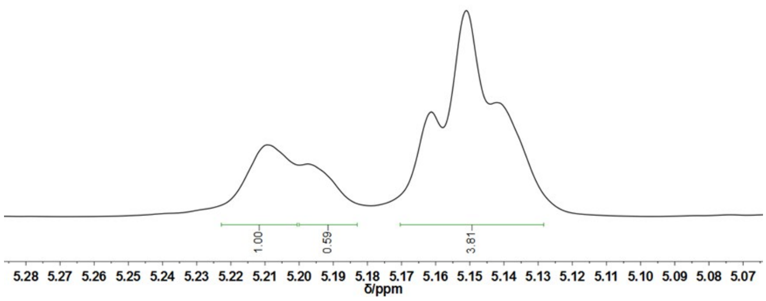

Fig. S39. Homonuclear decoupled ^{1}H NMR spectrum (500 MHz, $CDCl_3$, 25°C) of the resultant PLA (Table 1, run 9).

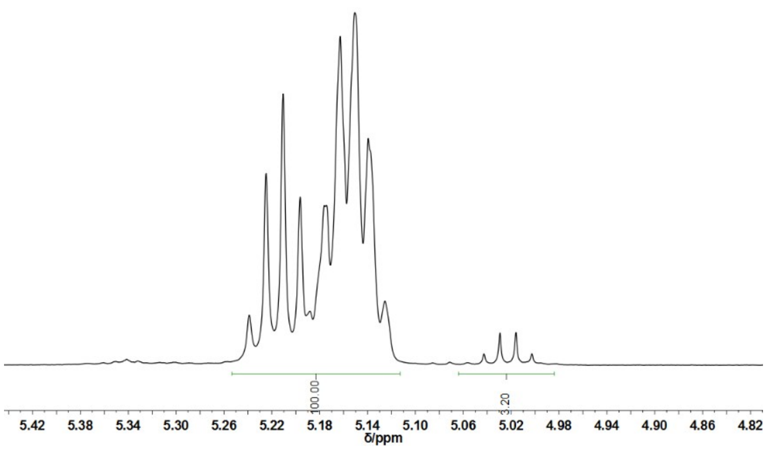

Fig. S40. ^{1}H NMR spectrum (500 MHz, $CDCl_3$, 25°C) of the resultant PLA (Table 1, run 10).

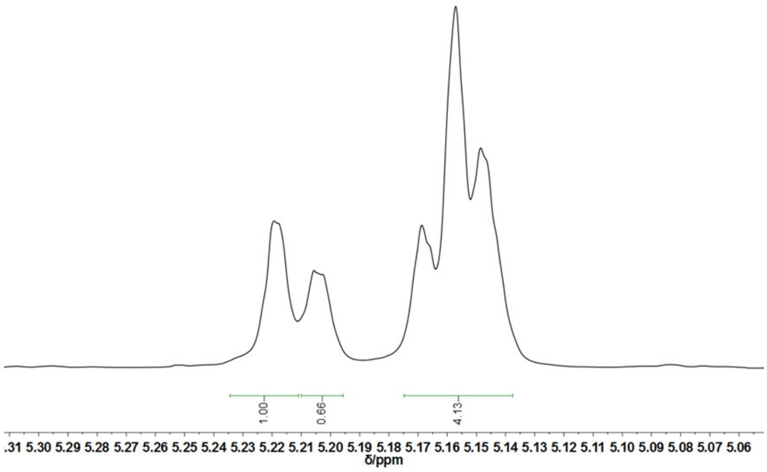

Fig. S41. Homonuclear decoupled ^{1}H NMR spectrum (500 MHz, $CDCl_3$, 25°C) of the resultant PLA (Table 1, run 10).

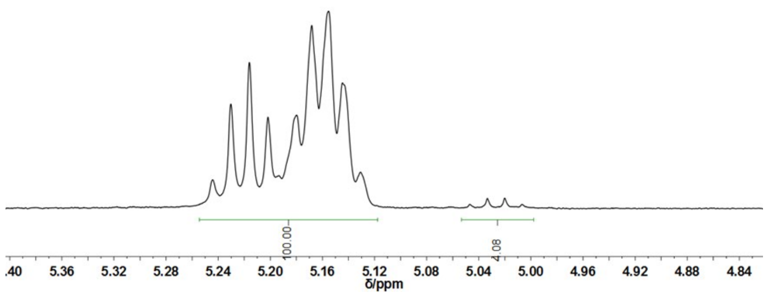

Fig. S42. ^{1}H NMR spectrum (500 MHz, $CDCl_3$, 25°C) of the resultant PLA (Table 2, run 1).

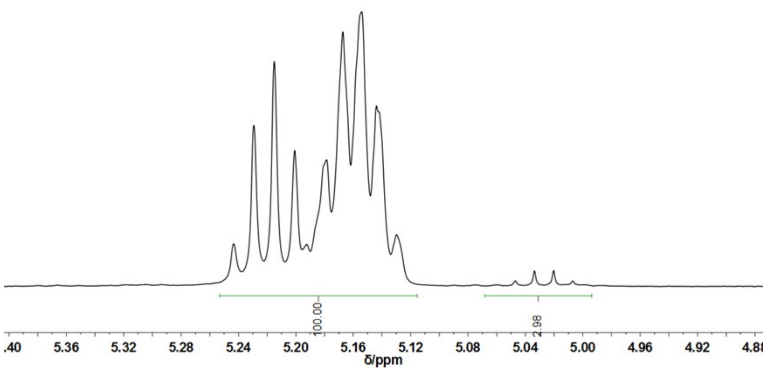

Fig. S43. ^{1}H NMR spectrum (500 MHz, $CDCl_3$, 25°C) of the resultant PLA (Table 2, run 2).

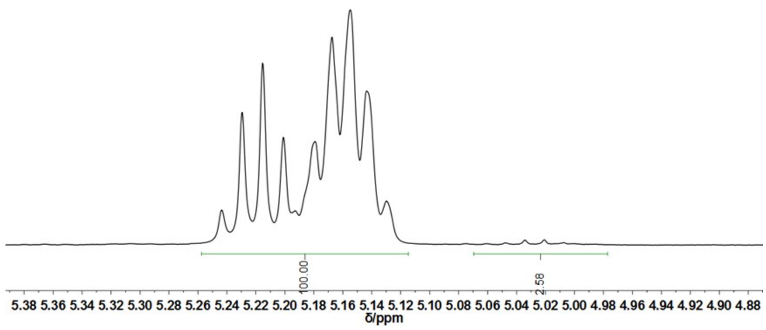

Fig. S44. ^{1}H NMR spectrum (500 MHz, $CDCl_3$, 25°C) of the resultant PLA (Table 2, run 3).

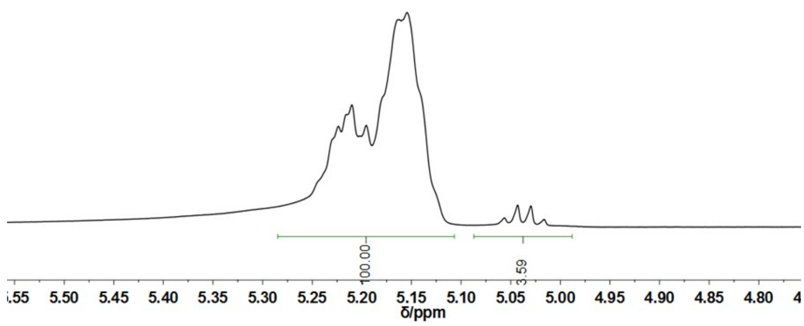

Fig. S45. ^{1}H NMR spectrum (500 MHz, $CDCl_3$, 25°C) of the resultant PLA (Table 2, run 4).

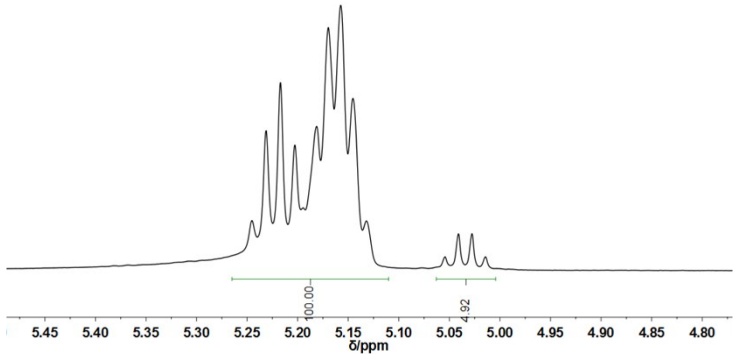

Fig. S46. ^{1}H NMR spectrum (500 MHz, $CDCl_3$, 25°C) of the resultant PLA (Table 2, run 5).

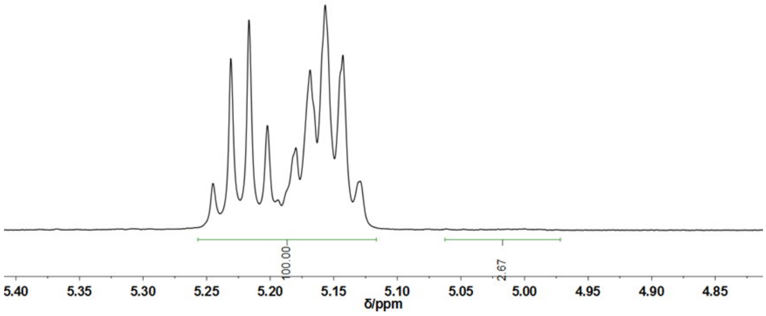

Fig. S47. ^{1}H NMR spectrum (500 MHz, $CDCl_3$, 25°C) of the resultant PLA (Table 3, run 1).

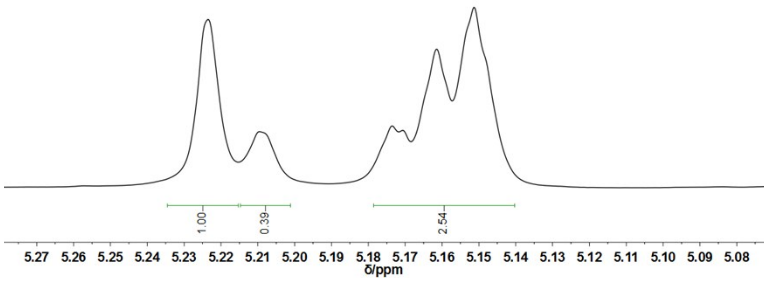

Fig. S48. Homonuclear decoupled ^{1}H NMR spectrum (500 MHz, $CDCl_3$, 25°C) of the resultant PLA (Table 3, run 1).

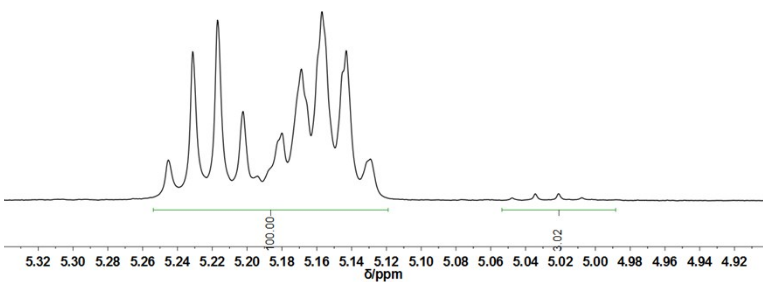

Fig. S49. ^{1}H NMR spectrum (500 MHz, $CDCl_3$, 25°C) of the resultant PLA (Table 3, run 2).

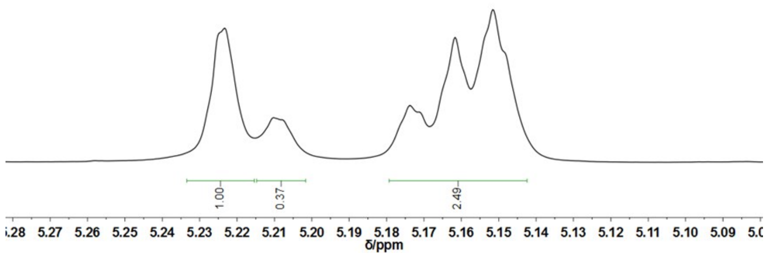

Fig. S50. Homonuclear decoupled ^{1}H NMR spectrum (500 MHz, $CDCl_3$, 25°C) of the resultant PLA (Table 3, run 2).

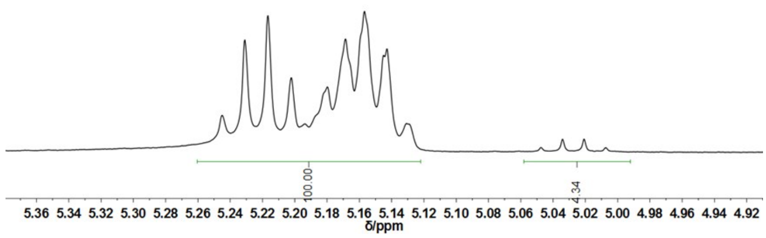

Fig. S51. ^{1}H NMR spectrum (500 MHz, $CDCl_3$, 25°C) of the resultant PLA (Table 3, run 3).

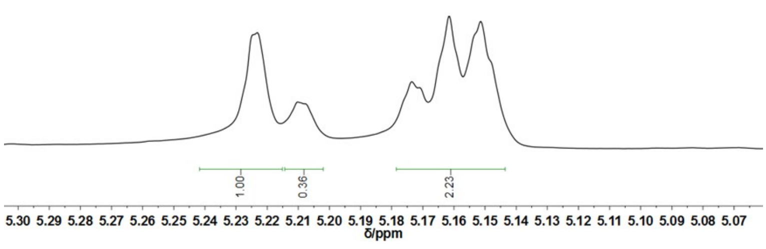

Fig. S52. Homonuclear decoupled ^{1}H NMR spectrum (500 MHz, $CDCl_3$, 25°C) of the resultant PLA (Table 3, run 3).

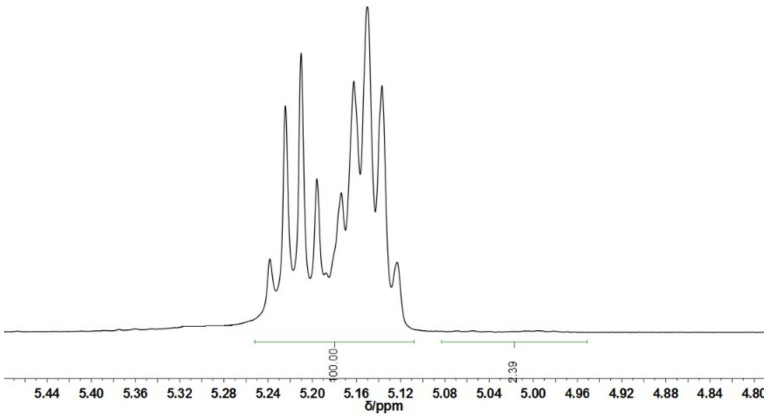

Fig. S53. ^{1}H NMR spectrum (500 MHz, $CDCl_3$, 25°C) of the resultant PLA (Table 3, run 4).

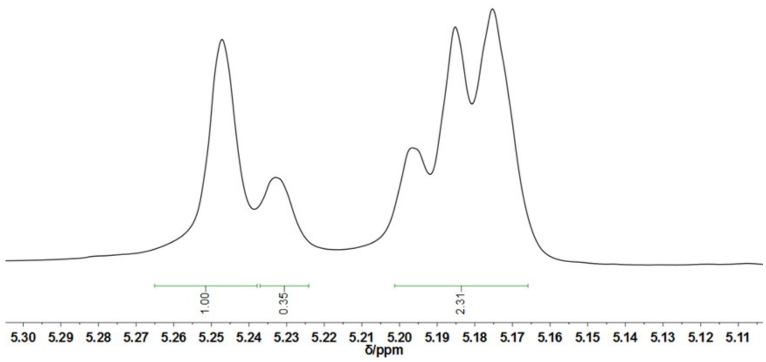

Fig. S54. Homonuclear decoupled ^{1}H NMR spectrum (500 MHz, $CDCl_3$, 25°C) of the resultant PLA (Table 3, run 4).

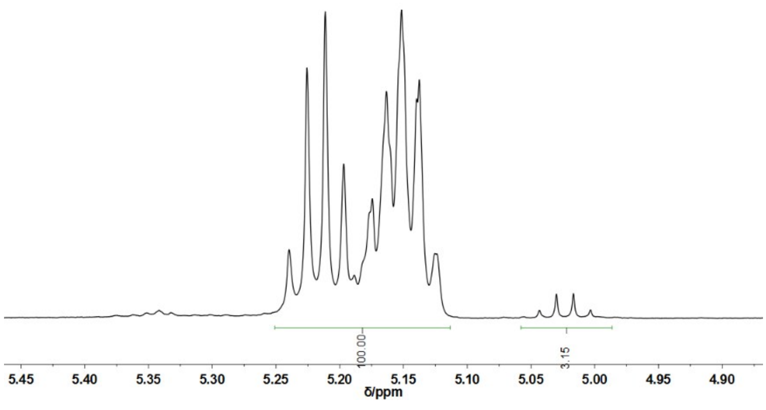

Fig. S55. ^{1}H NMR spectrum (500 MHz, $CDCl_3$, 25°C) of the resultant PLA (Table 3, run 5).

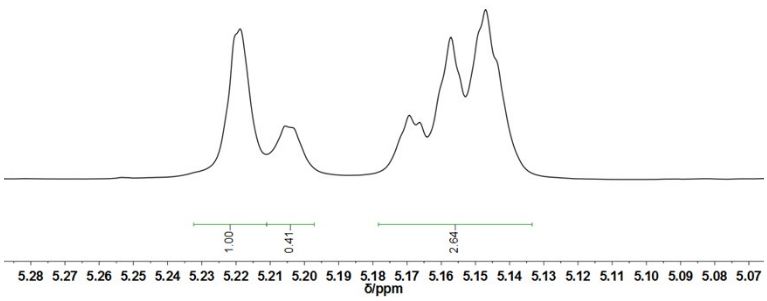

Fig. S56. Homonuclear decoupled ^{1}H NMR spectrum (500 MHz, $CDCl_3$, 25°C) of the resultant PLA (Table 3, run 5).

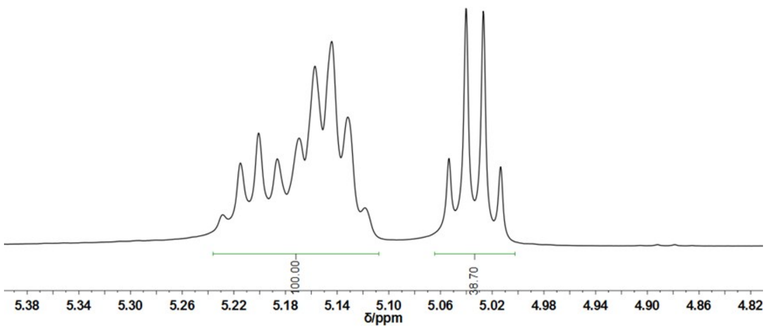

Fig. S57. ^{1}H NMR spectrum (500 MHz, $CDCl_3$, 25°C) of the resultant PLA (Table 3, run 6).

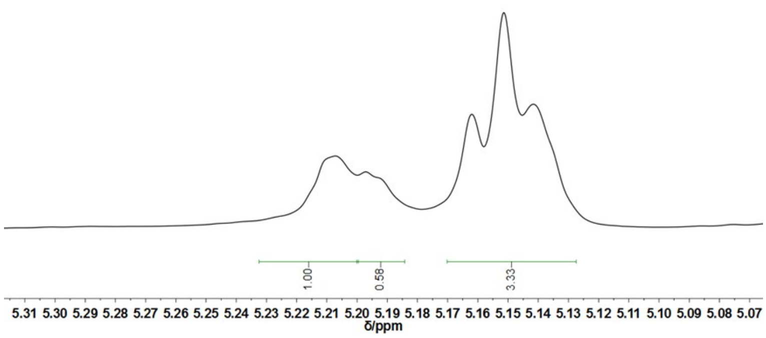

Fig. S58. Homonuclear decoupled ^{1}H NMR spectrum (500 MHz, $CDCl_3$, 25°C) of the resultant PLA (Table 3, run 6).

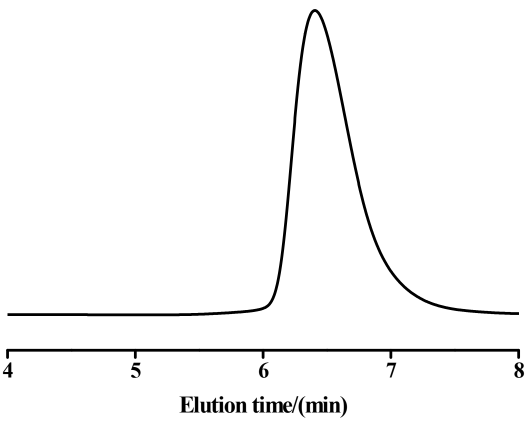

Fig. S59. The SEC trace of the resultant PLA (Table 1, run 1).

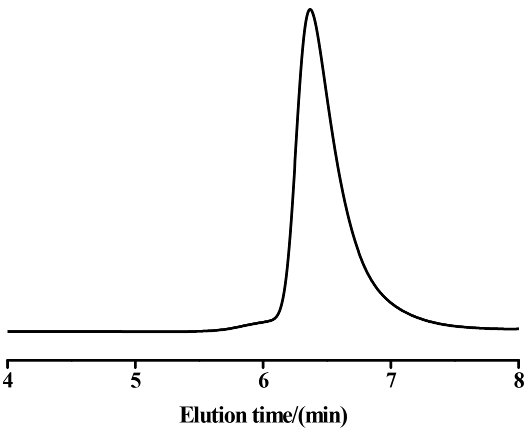

Fig. S60. The SEC trace of the resultant PLA (Table 1, run 2).

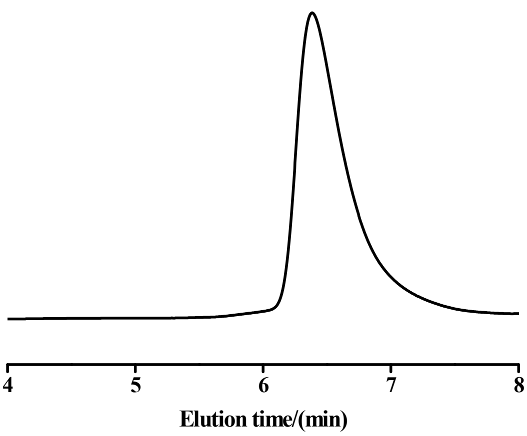

Fig. S61. The SEC trace of the resultant PLA (Table 1, run 3).

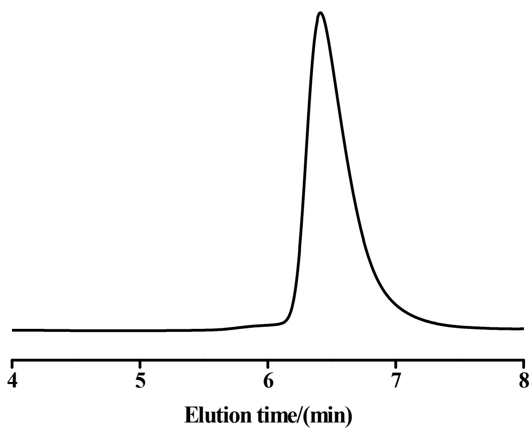

Fig. S62. The SEC trace of the resultant PLA (Table 1, run 4).

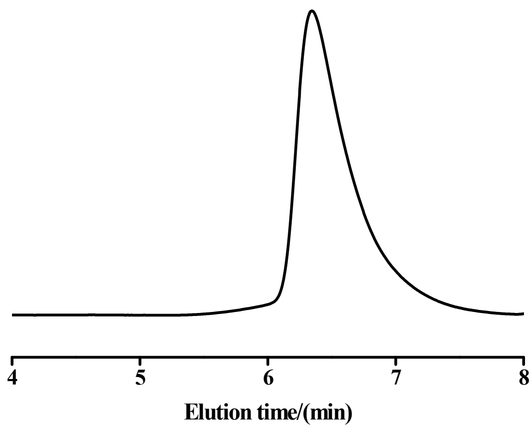

Fig. S63. The SEC trace of the resultant PLA (Table 1, run 5).

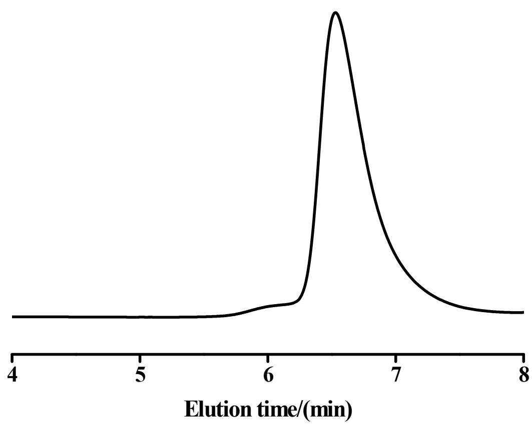

Fig. S64. The SEC trace of the resultant PLA (Table 1, run 6).

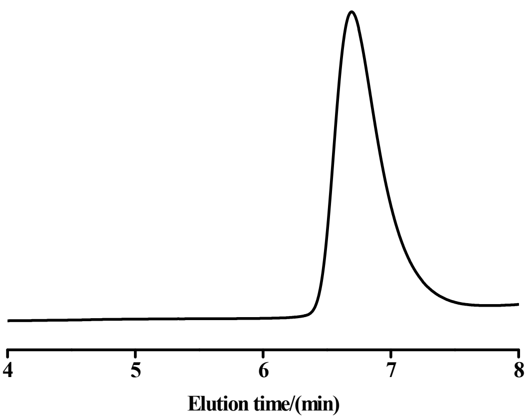

Fig. S65. The SEC trace of the resultant PLA (Table 1, run 7).

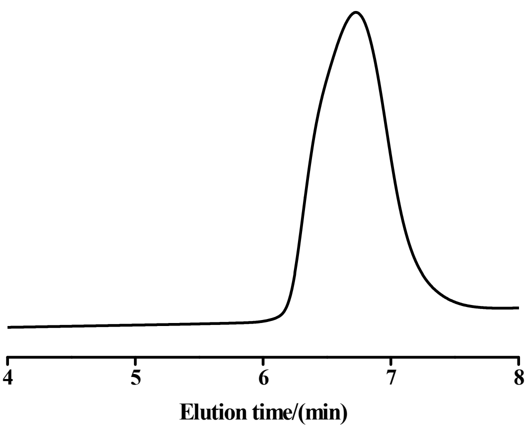

Fig. S66. The SEC trace of the resultant PLA (Table 1, run 8).

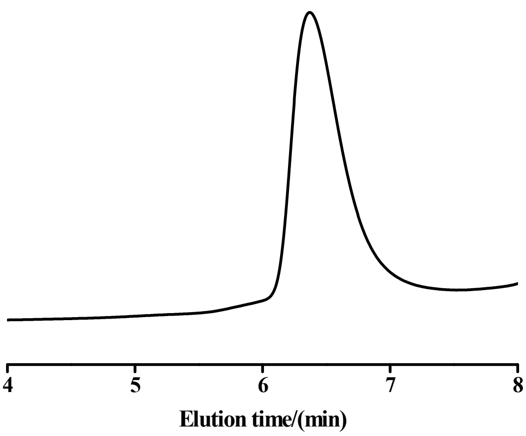

Fig. S67. The SEC trace of the resultant PLA (Table 1, run 9).

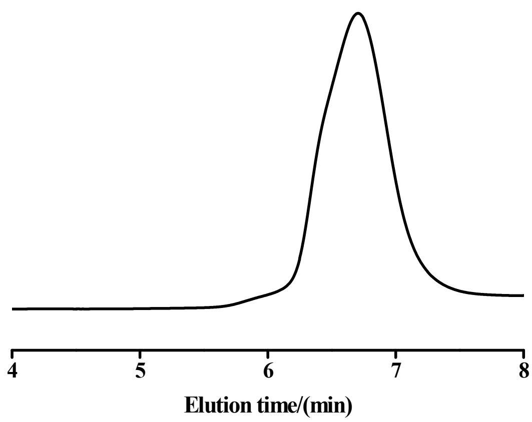

Fig. S68. The SEC trace of the resultant PLA (Table 1, run 10).

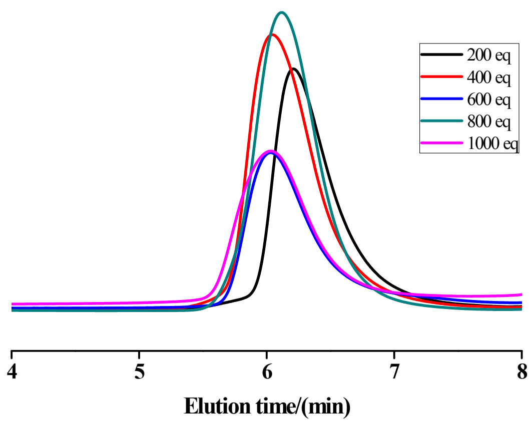

Fig. S69. The SEC traces of the resultant PLAs (Table 2).

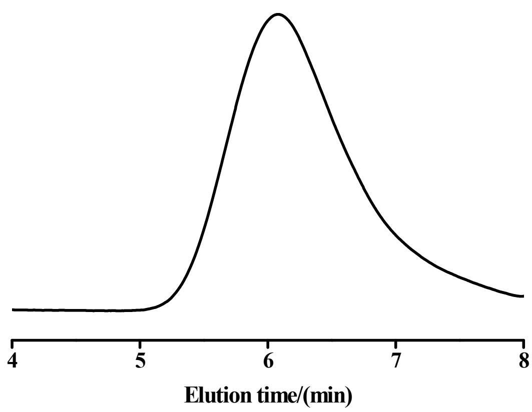

Fig. S70. The SEC trace of the resultant PLA (Table 3, run 1).

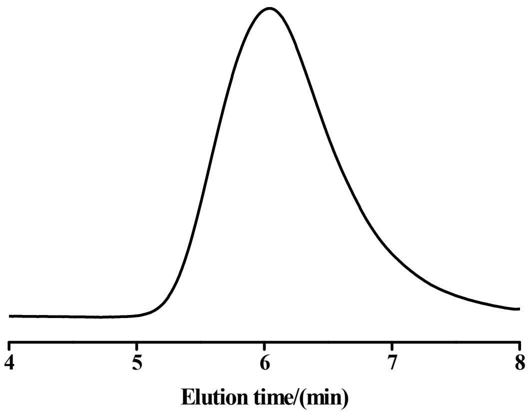

Fig. S71. The SEC trace of the resultant PLA (Table 3, run 2).

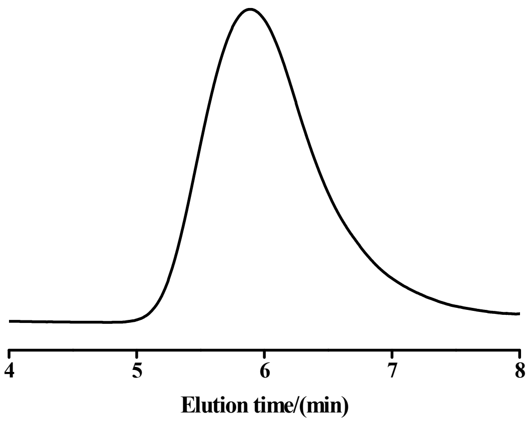

Fig. S72. The SEC trace of the resultant PLA (Table 3, run 3).

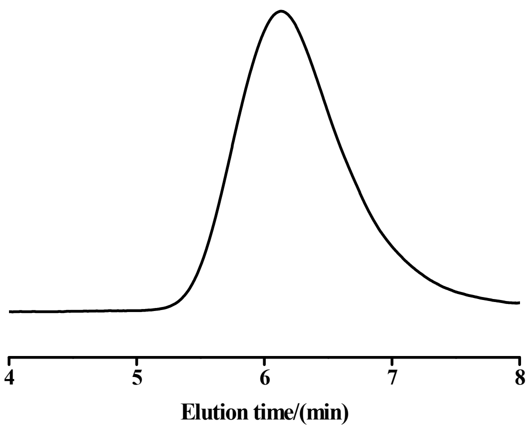

Fig. S73. The SEC trace of the resultant PLA (Table 3, run 4).

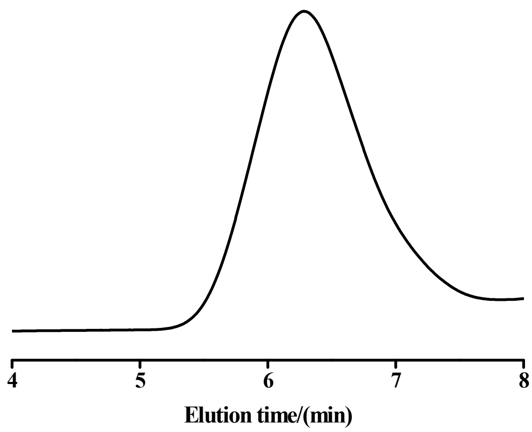

Fig. S74. The SEC trace of the resultant PLA (Table 3, run 5).

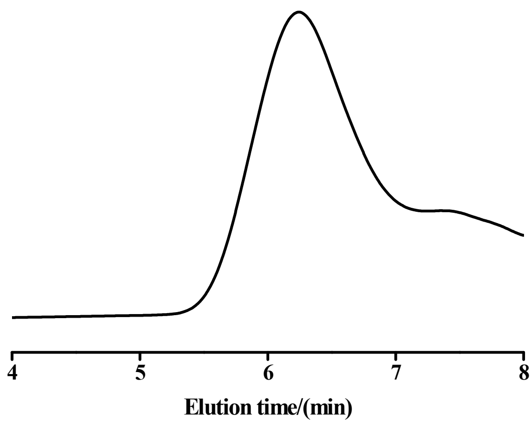

Fig. S75. The SEC trace of the resultant PLA (Table 3, run 6).